Polystyrene micro- and nanoplastics induce growth and physiological alterations in marine plants (seagrasses)

Virginia Menicagli[1,2†], Monica Ruffini Castiglione[3,4†], Elena Balestri[1*], Lucia Giorgetti[5], Stefania Bottega[3], Carlo Sorce[3,4], Carmelina Spanò[3,4§], Claudio Lardicci[2,4,6§]

[1]Department of Biology, University of Pisa, via Derna 1, 56126 Pisa, Italy

[2]Center for Instrument Sharing University of Pisa (CISUP), University of Pisa, via S. Maria 53, Pisa, Italy

[3]Department of Biology, University of Pisa, via L. Ghini 13, 56126 Pisa, Italy

[4]Center for Climate Change Impact, University of Pisa, Via Del Borghetto 80, Pisa, Italy

[5]Institute of Agricultural Biology and Biotechnology, (IBBA-CNR), Pisa, Italy

[6]Department of Earth Sciences, University of Pisa, via S. Maria 53, Pisa, Italy

**Corresponding author*

elena.balestri@unipi.it

† V. Menicagli and M. Ruffini Castiglione equally contributed

§ C. Spanò and C. Lardicci equally contributed

Abstract

Micro(nano)plastics are ubiquitous in marine environments and adversely affect wildlife. Yet the impact of these emerging pollutants on habitat-former species like seagrasses is still unknown. The present work explored the effects of short-term exposure (12 days) of seagrasses to an environmentally relevant concentration of polystyrene microplastics (MPs, 500 nm diameter) and nanoplastics (NPs, 30 nm diameter) on plant growth, oxidative status, and photosynthetic efficiency using *Cymodocea nodosa* as a model. Among plant organs, adventitious roots were particularly affected by MP/NPs showing complete degeneration. Total leaf number per shoot was lower for MPs- and NPs-treated plants compared to control, and for MPs-treated plants leaf loss exceeded leaf production. Moreover, MPs, probably due to their ability to adhere on plant surface, reduced photochemical efficiency compared to controls while increased pigment content. NPs, detected inside plant tissues by scanning microscopic observations, elicited the greatest oxidative damage also when, as in shoots, they induced higher phenol content than in control and MPs-treated plants. Biochemical data about oxidative stress markers were consistent with histochemical results. Our findings provide the first experimental evidence of the impact of MP/NPs on marine rooted plants and the potential risks these particles could pose to seagrass ecosystems and their functioning.

Keywords: marine litter, *Cymodocea nodosa*, phytotoxicity, oxidative stress, photosynthetic efficiency, nanoparticles

Highlights

1. For the first time micro-(MPs) and nanoplastics (NPs) were tested on seagrasses.
2. MPs and NPs adversely affected seagrass growth by increasing leaf loss rate.
3. MPs and NPs increased seagrass oxidative stress and affected phenol production.
4. MPs negatively affected seagrass photosynthetic machinery.
5. MPs and NPs could be a novel threat to marine ecosystems.

Graphical Abstract

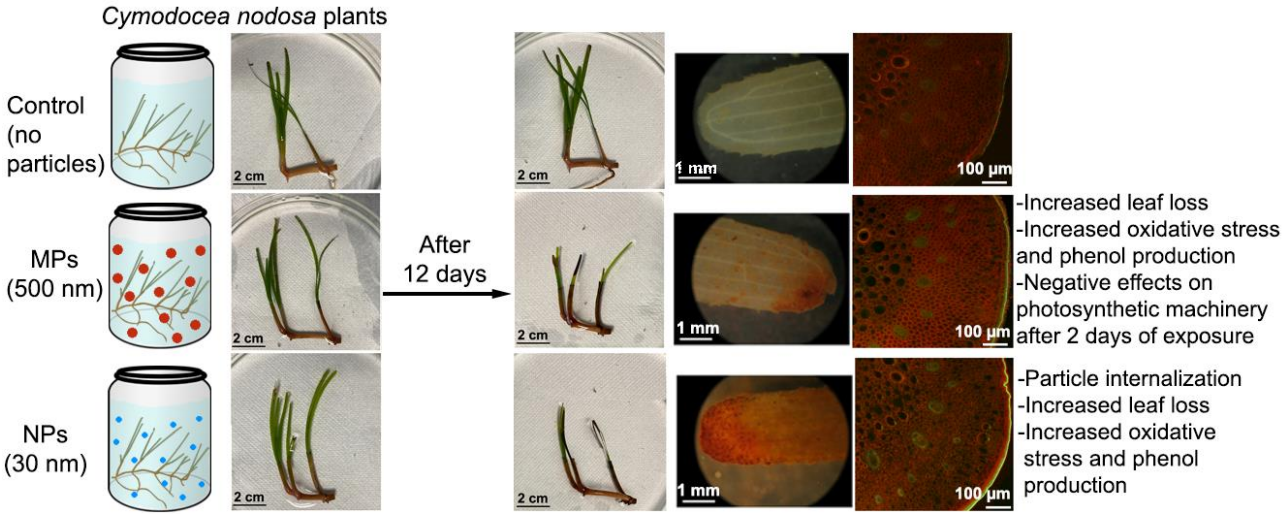

1. Introduction

Plastic waste is now present in all marine habitats (Eriksen et al., 2014; Bergmann et al., 2015), and the risks posed by this pollutant to marine wildlife, environments, and human well-being are globally recognized (Thompson et al., 2009; Bergman et al., 2015). Estimates indicate that more than 5 trillion pieces of plastic debris are floating in oceans (Eriksen et al., 2014). A relevant portion of this waste is constituted by small particles made of polyolefins, basically polyethylene, polypropylene, and polystyrene (Koelmans et al., 2015; Gangadoo et al., 2020) of variable size, such as microplastics (i.e., particles with a size from 100 nm to 1000 μm, MPs; Koelmans et al., 2015) and nanoplastics (from 1 to 100 nm, NPs; Koelmans et al., 2015; Hartmann et al., 2019). These particles mainly originate from the gradual breakdown and degradation due to weathering (e.g., thermal-, photo- and chemical-degradation) of plastic debris (Andrady, 2011; Koelmans et al., 2015), but they can also enter marine habitats directly at the small-scale size via the unintentional release from a variety of processes and products (e.g., cosmetics, paints, biomedical and electronic devices; da Costa et al., 2016; Blair et al., 2017). Concentrations of MPs can range on average from 1.4 μg/L to 7 μg/L in the Mediterranean Sea (Beiras and Schönemann, 2020) and from 0.013 to 100 particles/L in the oceans (Cao et al., 2022), and predictions indicate that these values will increase up to four times by 2060 (Isobe et al., 2016). There is still much uncertainty on the actual quantity of NPs in marine environments due to the lack of standardized techniques for sampling, characterizing, and analysing these particles (Gangadoo et al., 2020; Gao et al., 2021). Recent estimates suggest that NPs concentrations could be up to 10^{14} times higher than MPs ones (Besseling et al., 2019), and even larger in compartments suffering from high plastic pollution, such as coastal shallow near-shore habitats (Lenz et al., 2016; Gerstenbacher et al., 2022). Therefore, the possible negative impact raised by these emerging contaminants on marine organisms is of particular concern.

Available data indicate that MP/NPs can negatively affect marine wildlife by altering for example the feeding activity, growth, reproduction, and survival of fishes and filter-feeder organisms (Chae and An, 2017; Ferreira et al., 2019; Gangadoo et al., 2020; Gonçalves and Bebianno, 2021). However, the impact of these pollutants on photosynthetic primary producers, which are at the bottom of marine food-webs, is still relatively poorly known. Studies on the exposure of microalgae to MPs have shown contrasting effects, revealing from one side no impacts on growth and photosynthesis (see for example Long et al., 2017; Garrido et al., 2019; Mateos-Cárdenas et al., 2019) and on the other side growth inhibition (generally at very high concentrations) and a decreased chlorophyll content and photosynthetic efficiency (Zhang et al., 2017; Zhao et al., 2019). Adverse effects of NPs exposure on microalgae, such as alterations of growth and photosynthetic activity, increased production of intracellular reactive oxygen species (ROS) and reduced chlorophyll content, have also been reported (Bhattacharya et al., 2010; Besseling et al., 2014; Sjollema et al., 2016; Bergami et al., 2017; Gao et al., 2021). It has been hypothesized that MPs could act through various mechanisms including physical adhesion of particles on cell surface, blockage of entering light and nutrients, and increased water turbidity while NPs could damage cell membrane structure and DNA (Liu et al., 2020; Gao et al., 2021; Larue et al., 2021). The leaching of toxic additives from plastics could also play a role (Luo et al., 2019; Capolupo et al., 2020). However, the magnitude of MP/NP effects on marine organisms can vary according to their properties (e.g., polymer type, size, shape, surface functionalization, and charge of particles) and environmental conditions (e.g., temperature and salinity; Corsi et al., 2020). For example, greater negative effects have generally been observed with smaller-sized particles (Sjollema et al., 2016; Gao et al., 2021; Larue et al., 2021) and with positively charged and neutral NPs (Corsi et al., 2020; Gao et al., 2021; Gonçalves and Bebianno, 2021). Instead, less adverse effects on marine organisms have been found at high temperature due to reduced NPs bioavailability via induction of particle aggregation (Corsi et al., 2020).

Surprisingly, the potential impact of MP/NPs on marine rooted plants (seagrasses) has not been assessed yet. This is a relevant knowledge gap as an increasing number of studies indicates that seagrass meadows can act as a long-term sink for MPs due to their ability to trap particles and accumulate them in sediments (Goss et al., 2018; Cozzolino et al., 2020; Huang et al., 2020; Jones et al., 2020; Seng et al., 2020; Dahl et al., 2021; De los Santos et al., 2021; Sanchez-Vidal et al., 2021; Navarrete-Fernández et al., 2022). There is also evidence that the presence of epiphytes growing on seagrass leaves can play a role in promoting MPs accumulation (Goss et al., 2018; Gerstenbacher et al., 2022). Once in marine sediments, MPs can affect microbial communities leading to nutrient cycling alterations (Seeley et al., 2020) and increase locally the concentration of sediment pollutants acting as a vector for heavy metals and residual monomers (Cauwenberghe et al., 2015; Li et al., 2020a). Therefore, MP/NPs could interact with seagrasses both at shoot level via the aquatic medium and at root level via the sediment (Gerstenbacher et al., 2022). Experimental evidence indicates that in terrestrial and freshwater angiosperms, which share some anatomical traits with seagrasses, small MPs (200 nm) and NPs can be adsorbed by roots, accumulate in plant tissues and eventually be translocated to shoots, leading to multiple toxic effects, such as increased oxidative stress, DNA damage, gene expression alterations, reduction of photosynthesis and inhibition of seed germination (Bosker et al., 2019; Giorgetti et al., 2020; Sun et al., 2020; Mateos-Cárdenas et al., 2021; Lian et al., 2022; Spanò et al., 2022). Seagrass meadows provide a wide range of fundamental ecosystem services, like nutrient cycling regulation, nursery habitat provisioning, and coastal protection (Barbier et al., 2011), but they are under threat globally due to anthropogenic impacts and climate-change-related stressors (Orth et al., 2006; He and Silliman, 2019). Thus, an evaluation of the potential risks posed by MPs and NPs to seagrass ecosystems is critically important.

In the present study, we investigated the effects of the exposure of seagrasses to an environmentally relevant concentration of MPs (500 nm diameter particles) and NPs (30 nm diameter particles) made of polystyrene (PS). As a model, we selected *Cymodocea nodosa* (Ucria)

Ascherson, a fast-growing pioneer species which forms monospecific and mixed meadows along the Mediterranean and Atlantic coasts and provides important ecosystem services (Cabaco et al., 2010). This seagrass is considered as a useful bioindicator organism due to its ability to concentrate pollutants and silver nanoparticles in some organs (Mylona et al., 2020a). It was also proven as a useful species for testing the effects of plastic items on seagrasses (Balestri et al., 2017; Balestri et al., 2019; Menicagli et al., 2021). Specifically, we investigated under laboratory conditions whether a short-term (12 days) exposure of plants to MP/NPs induced lethal (e.g., plant mortality) or sub-lethal toxic effects (e.g., reduced growth, and alterations of photosynthetic efficiency and oxidative stress). Scanning Electron Microscopy (SEM) analysis was performed to evaluate the possible absorption of PS particles and internalization in plant tissues.

2. Materials and methods

2.1 Polystyrene nanoparticles

Non-functionalized red died PS spheres of nominal size 30 nm and 500 nm (PS density 1.06 g/cm^3) supplied as 1% solid suspension (10 mg/mL) were purchased from Phosphorex, Inc (South St. Hopkinton (MA), USA). These spheres were used as a proxy for plastic pollution. To verify the real size of NPs and MPs, a drop (10 µL) of particle suspension diluted 1:20 was placed on a coverslip. The suspension was allowed to dry, and, after critical point drying, particles were coated with gold and examined with scanning electron microscope (SEM, JSM-5410, Jeol, Tokyo, Japan). Captured images were assessed by the ImageJ programme (Image J 1.52a, National Institutes of Health, USA, http://imagej.nih.gov/ij) to measure the diameters of at least 300 particles of MPs and NPs.

2.2 Plant collection and culture conditions

At the end of May 2021, plagiotropic (horizontal) rhizomes of *C. nodosa* bearing an apical meristem and shoots (runners) were randomly collected from a shallow meadow of Italy, Ligurian

Sea (43° 22′ 55.66″ N, 10° 26′ 7.05″ E). This locality is characterized by oligotrophic waters with constant salinity (38 psu). Rhizomes were collected at a depth of 0.5 m, rinsed with natural seawater (NSW) at the sampling site and then transported to the laboratory. Here, they were cut with a scissor to achieve homogeneous sized plant units (i.e., approximately 4 cm rhizome length, 2-4 shoots and 0-2 roots), and each unit was placed in a 100 mL sterilized glass culture vessel filled with a growth medium consisting of NSW enriched with nutrients supplied as a commercial NPK fertilizer (Cifo, 20-10-10, 0.44 g/L). Salinity and pH of the NSW-based growth medium, measured using a multiparameter meter (HI98194, Hanna Instruments), were 38.10 ± 0.05 and 7.96 ± 0.01, respectively. NSW was provided by the INVE Aquaculture Research Center of Rosignano Solvay, which collected the water from an oligotrophic area (ARPAT, 2014) near to the seagrass sampling site: this water was continuously filtrated by using two consecutive GAV filters (RBXPL type, 1 µm mesh) and treated with ozone and UV lamps (GSW1 type berson) for sterilization. Before performing the exposure test, plants were kept in a conditioning room to acclimate for 7 days under environmental conditions (23.3 ± 0.1°C, mean ± SE, 12/12 h photoperiod and 122.54 ± 32.54 µmol m^{-2} s^{-1}mean daily photon flux density) close to those experienced in the field by the species during the season of most rapid growth (May-August, Duarte and Sand-Jensen, 1990). Our preliminary tests have demonstrated that this cultivation system can allow the growth of *C. nodosa* for at least 4 weeks.

2.3 Plant exposure to polystyrene nanoplastics

After acclimatization, *C. nodosa* plants were transferred individually in sterilized glass vessels filled with one of the two test media, NPs or MPs. These media were prepared by adding a volume of PS stock solution, either NPs or MPs, to 90 mL of NSW-based medium to obtain a final concentration of 68 µg/L, corresponding to approximately 4.5 x 10^{12} particles/L for 30 nm NPs and 9.8 x 10^{8} particles/L for 500 nm MPs (Leusch and Ziajahromi, 2021). This concentration was in the range of those used in PS NPs toxicity tests on microalgae and considered as environmentally relevant (Cao

et al., 2022). Plants kept in the NSW-based growth medium without PS stock solution were used as negative controls. All vessels were agitated on an orbital shaker (at 70 rpm) for 10 min before adding the plants. There were 16 replicates for each treatment, 48 plants in total. The vessels were arranged in the conditioned room and left under the same environmental conditions described previously for the plant acclimatization period. Vessel position was regularly changed (approximately twice a day) during the experiment to minimize spatial micro-environmental variations of light and temperature among vessels. The medium in each vessel was aerated twice for 1 hour every day using aquarium air pumps to improve oxygen supply and provide seawater motion. Deionized water (LiChrosolv LC-MS grade, Merck) was added when necessary to minimize salinity variations and restore water level dropped due to evaporation over the experimental period. The test medium in each vessel was completely renewed 7 days after the beginning of the experiment. During the experiment, leaves naturally detached from shoots were gently removed from the medium using cleaned sterilized tweezers. Plants were visually checked at short-term (2 days after the start of the experiment) and at mid-term (7 days after the start of the experiment) for shoot/leaf production and mortality. SEM observations, final plant growth measurements, and evaluation of oxidative stress markers on plant organs were performed after 12 days of exposure, i.e., at the end of the experiment. Photosynthetic efficiency measurements were carried out both after 2 days and 12 days of exposure.

2.4 SEM observations of plants

For plant organ observations, fresh leaves and rhizomes excised from three samples of treated and control plants were cut into small pieces, fixed in 3% glutaraldehyde in 100 mM sodium phosphate buffer (pH 7.4) for 24 h and then processed as previously described (Spanò et al., 2019). After critical-point drying, both leaves and rhizomes blocks were cross sectioned, coated with gold and examined and captured with SEM (JSM-5410, Jeol, Tokyo, Japan) (Lian et al., 2020).

2.5 Plant growth responses

At the start of the experiment, the number of shoots, the number of leaves per shoot and the length of the intermediate leaf (i.e., the internal leaf without sheath) of all shoots in *C. nodosa* plants were recorded. Analysis of these variables did not show significant differences between plants assigned to different treatments (Table S1, Fig. S1). The measurement of such variables was repeated at the end of the experiment to evaluate the effects of exposure to plastic particles on plant performance, in terms of mortality, net change in shoot number per plant and leaf number per shoot, and leaf elongation rate. The effects of MPs and NPs on plant growth were examined on 12 plants per treatment. Net change in shoot number per plant was calculated as difference between the number of newly produced shoots and those died during the experimental period. Similarly, net change in leaf number per shoot was calculated as the difference between the number of newly produced leaves and those died averaged across all shoots of each plant during the experimental period. Negative values indicated that shoot (or leaf) recruitment did not balance shoot (or leaf) mortality suggesting a decline of plant growth. Positive values indicated that shoot (or leaf) recruitment exceeded mortality reflecting plant growth, while a zero-value indicated that mortality was balanced by recruitment resulting in a steady plant state. Leaf elongation rate (cm $leaf^{-1}$ day^{-1}) was also calculated as difference between the final length (cm) and the initial length of the intermediate leaf of each shoot divided by 12. Toxicity index (TI, %), based on the mean final number of leaves per shoot was also calculated according to the following formula: $TI = [(LPSC – LPST) / LPSC] * 100$, where LPSC is the final number of leaves per shoot in the control and LPST is the final number of leaves per shoot in a plastic treatment (Mylona et al., 2020b, modified).

2.6 Extraction and determination of hydrogen peroxide and thiobarbituric acid reactive substances (TBARS)

Hydrogen peroxide content of shoots and rhizomes was determined according to Jana and Choudhuri (1982). After extraction with phosphate buffer 50 mM pH 6, the homogenate was centrifuged at

6,000g for 25 min and mixed with 0.1% titanium chloride in 20% (v/v) H_2SO_4. After centrifugation (6000g for 15 min) the absorbance of supernatant was read at 410 nm. The concentration of H_2O_2 was calculated from a standard curve and expressed as μmol g^{-1}FW. Lipid peroxidation was estimated in terms of TBARS according to Wang et al. (2013) with minor modifications (Spanò et al., 2017). The concentration of TBARS was estimated measuring the specific absorbance at 532 nm and subtracting the non-specific absorbance at 600 nm and expressed as nmol g^{-1}FW. Calculation was made basing on an extinction coefficient of 155 mM^{-1} cm^{-1}.

2.7 Extraction and determination of phenols and photosynthetic pigments

Phenolic compounds were measured in shoots and rhizomes according to Arezki et al. (2001). After homogenization in HCl 0.1 N, phenolic extracts were left at 20 °C for 3 h. 300 μL of extract were added to 1.5 mL H_2O + 0.1 mL Folin–Ciocalteu reagent and left so for 3 min. After addition of 400 μL Na_2CO_3 (20% w/v) and incubation at 100 °C for 1 min, the samples were cooled in ice bath and the absorbance at 750 nm was read. Phenolic compounds content was calculated as equivalent of gallic acid (GAE mg g^{-1} FW) on the base of a standard calibration curve. Leaf chlorophylls (a, b, and total) and carotenoids were extracted and determined as in Spanò and Bottega (2016). The concentrations of pigments were expressed as mg g^{-1} FW.

2.8 Oxidative stress markers histochemical assays

Leaves of comparable size and length belonging to five plants randomly selected for each treatment were isolated and cut to obtain leaf tip and a mid-leaf portion. Histochemical detection of hydrogen peroxides was obtained by dipping leaf portions in staining solution containing 1 mg/mL DAB, pH 3.8, and vacuum infiltrating (Daudi and O'Brien, 2012). After 20 min the samples were incubated overnight in the same solution, lightened in 96% ethanol for 60 min at 65°C and then analysed under a light stereomicroscope to evaluate the presence of brown precipitates. *In situ* determination of lipid peroxidation was performed with Schiff's reagent (Yamamoto et al., 2001) (VWR Chemicals BDH)

that, binding to free aldehyde groups, can be considered a qualitative indicator of lipid peroxidation. Leaf portions were incubated with the dye for 60 minutes at room temperature, after that the samples were bleached in 96% ethanol for 60 min at 65°C. The samples were then analysed under a light stereomicroscope to evaluate the developed purple colour. For leaf histochemical assays a WILD Heerbrugg M420 stereomicroscope equipped with a Canon PowerShotS45 camera was employed. Rhizomes from the same five plants were cross sectioned with hand microtome. *In situ* detection of hydrogen peroxides was done according to Giorgetti et al. (2019) by Amplex UltraRed Reagent (Life Technologies, USA) that was applied to cross sections for detection of H_2O_2. After staining, slices were mounted in glycerol and observed with fluorescence microscope (568ex/681em nm). Lipid peroxidation levels were analysed with fluorescence microscope, as a change of the fluorescence emission peak from red to green, after staining with BODIPY 581/591 C11 probe (Life Technologies, USA) (Spanò et al., 2020). Microscope evaluation was performed acquiring simultaneously the green (485ex/510em nm) and the red fluorescence (581ex/591em nm) signals and merging the two images. Fluorescence microscope analysis was carried out with a Leica DMLB, equipped with appropriate set of excitation/emission filters and with a Leica DC300 ccd camera.

2.9 Photosynthetic efficiency

The overall functional efficiency of plants was investigated by the analysis of the biophysics of the photosynthetic light reactions, that are widely acknowledged as a sensitive index of stress (Kalaji et al., 2014), included that caused by NPs (Spanò et al., 2020). Such evaluation was performed by the measurement of photosystem II (PSII) fluorescence. This was recorded, at the start of the experiment (T = 0), after two days of treatment (T = 2) and at the end of the experiment (T = 12), by a chlorophyll fluorometer (Handy PEA, Hansatech Instruments, Ltd., Pentney, King's Lynn, UK) on three mature leaves per plant, previously acclimated to darkness for 20 min with a designated clip. Leaves were then exposed for 1 s to 3500 µmol photons m^{-2} s (650 nm peak wavelength) and chlorophyll a fluorescence was recorded. The three measurements taken on each plant were averaged to yield a

311 single value; four plants were measured for each treatment, and they were considered as independent
312 replicates. The fluorescence data were processed by PEA plus software (Hansatech Instruments),
313 which performed the analysis of the fast fluorescence kinetics (JIP test; Stirbet et al., 2018).
314
315 *2.10 Data analysis*
316 Statistical analyses were performed by using the statistical software "R" (version 3.5.2; R Core
317 Team, 2018). The effects of treatments (control, NPs, and MPs) on growth variables, oxidative
318 stress markers, and photosynthetic efficiency were assessed using one-way analysis of variance
319 (ANOVA, "GAD" package, Sandrini-Neto and Camargo, 2014). Prior to the analyses, data were
320 tested for normal distribution and homoscedasticity using Shapiro−Wilk test and Cochran test,
321 respectively. In cases of violation of assumptions, a Kruskal-Wallis test was used. The Tukey HSD
322 post-hoc test was conducted when significant differences ($p < 0.05$) among treatments were
323 observed.
324
325 **3. Results and Discussion**
326 *3.1 SEM analysis of micro(nano) particles and plants*
327 Figure 1a,b shows isolated NPs and MPs as observed under SEM. They showed a round profiled
328 shape and were often detectable as aggregates. NPs diameter varied from about 10 nm to 90 nm and
329 the most represented frequency classes were those from 21 to 30 and from 31 to 40 nm. MPs diameter
330 was between 200 and 600 nm with the most represented frequency class from 301 to 400 nm (Fig.
331 S2a-b).
332 Figure 1c,f shows a representative image of *C. nodosa* rhizome and leaf cross sections of control
333 samples, as processed for SEM analysis. In samples treated with NPs, SEM analysis allowed to
334 observe in the outer cortical tissues of rhizome (Fig. 1d,e) and in leaf mesophyll (Fig. 1g,h) the
335 presence of particles of a size and shape comparable to the NPs used for the treatment. These results
336 indicate that, in our experimental system, NPs seem to be able to cross epidermal tissues of both

leaves and rhizome. For leaves of *C. nodosa*, without stomatal apertures as occurs in seagrasses, it is possible to hypothesize a cuticular penetration of nanomaterials. Epidermal cells display a thin cuticle and subcuticular cavities (Kuo and den Hartog, 2006) and specific cell wall composition (Pfeifer and Classen, 2020), which probably facilitate the entry of NPs by altering the dynamic behaviour and the diameter of the cell wall pores. However, even in terrestrial plants, an entry of nanomaterials *via* aqueous pores of the leaf cuticle has been demonstrated, in parallel to the more widespread stomatal pathway (Larue et al., 2014) thus supporting our hypotheses. For rhizome the easiest way for NPs to entry could be the area corresponding to the damaged adventitious roots, without however excluding a penetration from the epidermal tissue. Further studies, with finer methodological approaches, will whatever be necessary to understand these mechanisms and above all if in this system NPs, once entered, can move from one organ of the plant to another.

Plant samples treated with MPs did not show particle internalization in analysed tissues of both rhizome and leaf. These results suggest that in our system MPs are not able to overcome plant barriers and spread into the plant tissues due to their dimensions. However, in accordance with Seng et al. (2020) they could adhere on plant surface (through encrustation and entrapment by associated epibionts, or sticky bacterial coatings) being in this way still capable, to some extent, of altering cellular physiology, as shown by the results below reported.

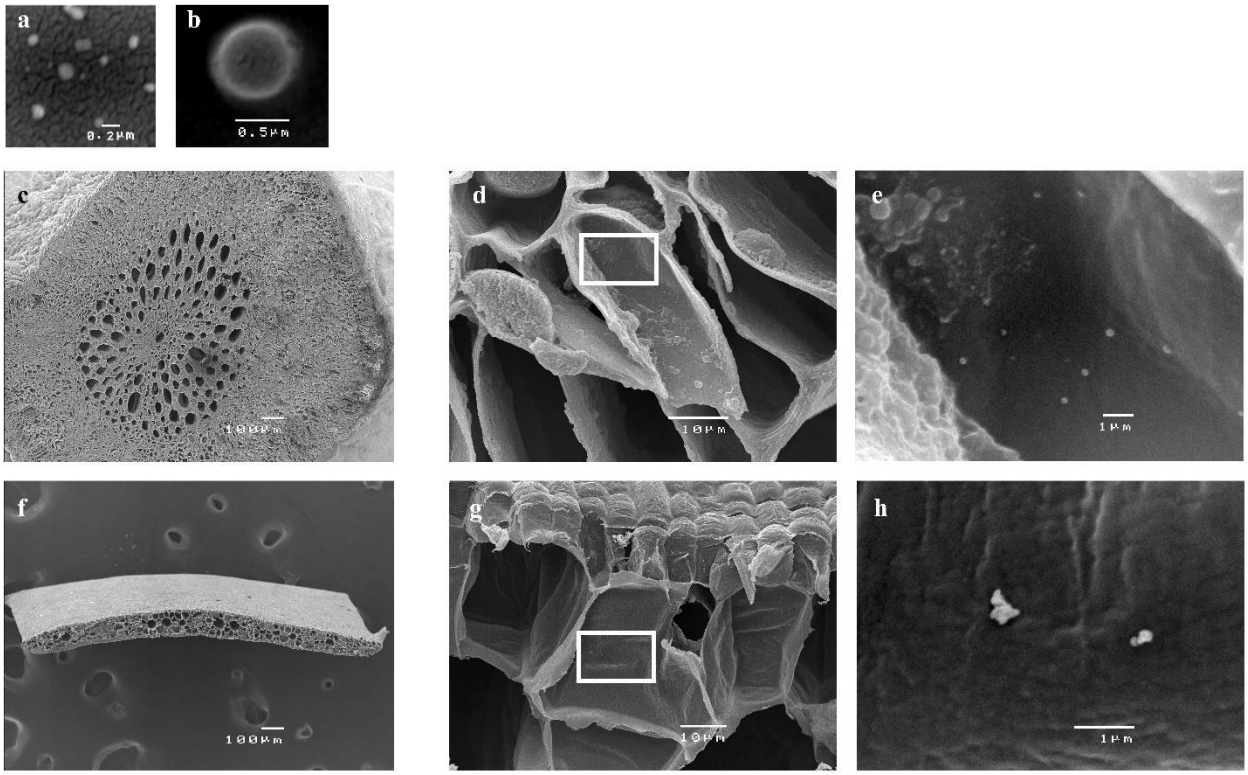

Fig. 1 Scanning electron microscopy (SEM) representative images of plastic polystyrene particles (a, NPs; b, MPs) and of *Cymodocea nodosa* plant samples as they appeared in microscopic analysis. (c) and (f) show a transversal cut of rhizome and leaf of control samples, (d) shows detail of rhizome cortex cells of NPs treated plants in which NPs were observed as single particles, (e) shows an enlargement of the pane in d, (g) shows a detail of leaf mesophyll cells of NPs treated plants in which NPs were observed as particle aggregates, and (h) shows an enlargement of the pane in g.

Two-column fitting image

3.2 Growth responses

All *C. nodosa* plants were alive at the end of the experiment. On average, the total number of shoots per plant did not differ among treatments (χ^2: 3.61, df = 2, $p > 0.05$; Fig. 2a). However, some shoots of plants grown with MPs and NPs died during the experiment and were partly replaced by newly produced shoots. Mean values of net change in shoot number were negative for plants grown with MPs and positive for control plants and those treated by NPs (Fig. 2b), but the analysis did not

389 detect significant differences among treatments (χ^2: 1.97, df = 2, p > 0.05). No difference in terms
390 of mean elongation rate of the intermediate leaf ($F_{2,33}$= 1.88, p > 0.05) was found among treatments
391 (Fig. 2c). This finding is not consistent with the elongation of leaves of *C. nodosa* after exposure to
392 other contaminants reported in previous studies (Adamakis et al., 2018; Mylona et al., 2020a), while
393 it agrees with the lack of relevant effects of PE MPs on the leaf growth rate of freshwater plants
394 (Kalčíková et al., 2017). In our study, no difference in terms of number of newly produced leaves
395 per shoot (χ^2: 3.25, df = 2, p > 0.05) was also detected among treatments (Fig. 2d). The leaf
396 elongation rate and the number of newly produced leaves per shoot observed in this study were
397 consistent with those detected by previous studies (Cunha and Duarte, 2007; Sghaier et al., 2011;
398 semmai mettere Adamakis et al., 2018 per elongation rate). ~~However,~~ Plants exposed to MPs and
399 NPs had a significantly lower total number of leaves per shoot than controls ($F_{2,33}$= 4.69, p < 0.05;
400 Fig. 2e and Fig. S3). Plants treated by MPs also showed a greater number of dead leaves per shoot
401 (χ^2: 6.36, df = 2, p < 0.05; Fig. 2f) and a lower net change in leaf number (χ^2: 8.26, df = 2, p < 0.05;
402 Fig. 2g), resulting in a leaf loss approximately 38% higher than controls. These results indicate that
403 neither MPs nor NPs affected leaf production process, but the former reduced the lifespan of adult
404 leaves. This was probably due to major exposure of these leaves to MPs particles, being at the
405 external of shoot, compared to intermediate or young leaves, and to the presence of epiphytes on
406 their surface. They also differ in their physiological status and response to abiotic stress from
407 intermediate and immature ones (Ruocco et al., 2019). Mean toxicity index based on the number of
408 leaves per shoot recorded in plants treated with NPs and MPs was approximately 23.2 ± 5.1 and
409 27.8 ± 8.6, respectively. These values are within the range of those observed for *C. nodosa* plants
410 exposed to silver nanoparticles and for other seagrass species treated by titanium dioxide
411 nanoparticles (Mylona et al., 2020a,b), and they could indicate moderate adverse plant growth
412 effects. They also agree with experimental evidence showing that MPs and NPs can negatively
413 influence aboveground organ development of terrestrial and freshwater rooted plants (Qi et al.,
414 2018; Boots et al., 2019; van Weert et al., 2019; Meng et al., 2021). During our experiment, the

roots of *C. nodosa* plants exposed to PS particles underwent tissue degeneration. Studies have reported that MPs and NPs can adversely affect the viability of root cells and decrease root activity in plants (Kalčíková et al., 2017; Yu et al., 2021; Zhou et al., 2021) probably through the absorption and accumulation of particles in roots (Dovidat et al., 2019; Jiang et al., 2019; Sun et al., 2020). Thus, MPs and NPs might interact with roots by adhering to them resulting in the mechanical damage of root cells.

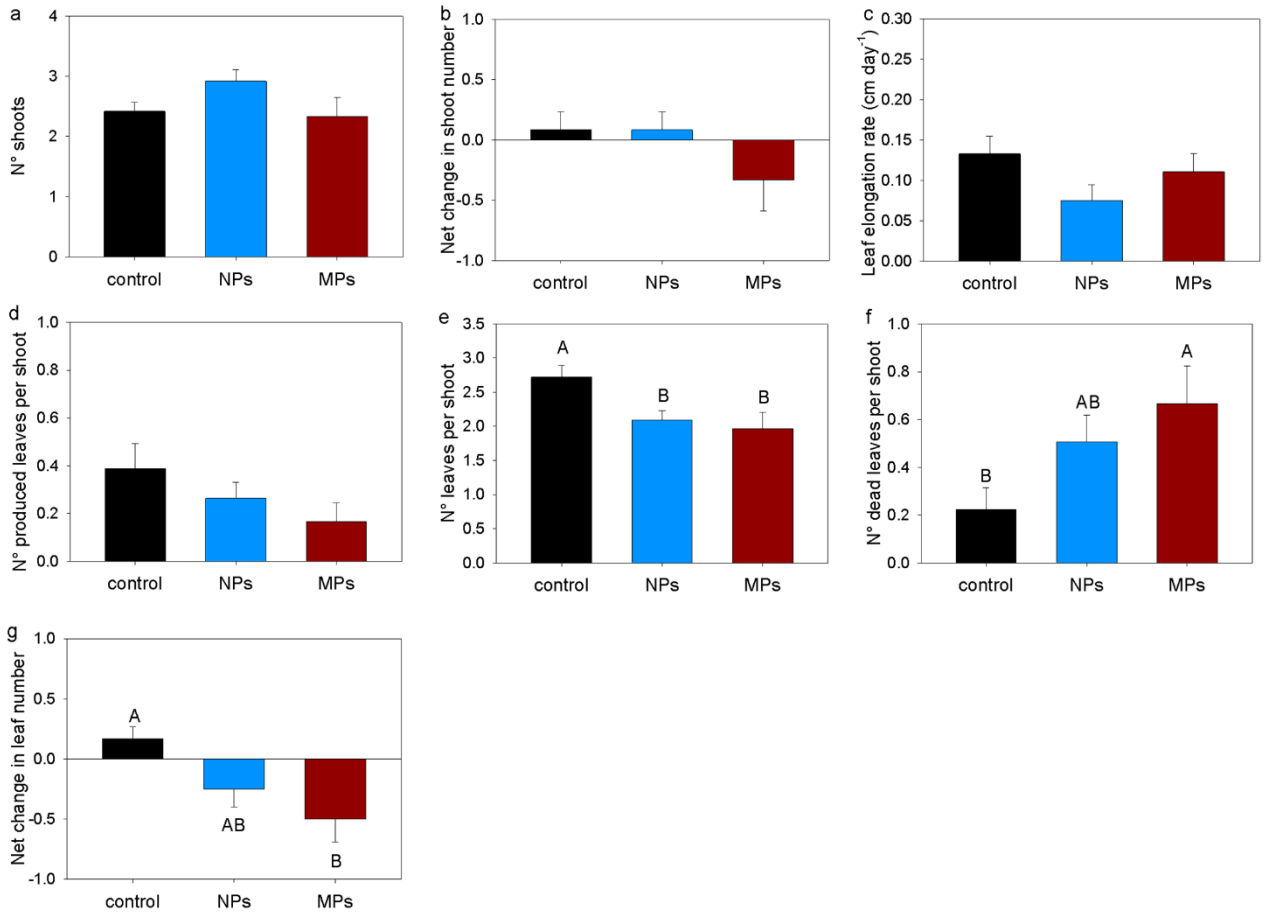

Fig. 2 (a) Final shoot number, (b) net change in shoot number, (c) elongation rate of the intermediate leaf, (d) number of produced leaves per shoot, (e) number of leaves per shoot, (f) number of dead leaves per shoot, and (g) net change in leaf number observed for *Cymodocea nodosa* plants grown without plastic polystyrene particles (control) or treated by NPs or MPs. Different letters above bars denote significant differences ($p < 0.05$) among treatments. Values are means ± SE. n = 12.

Two-column fitting image, color in online version only

441

442 *3.3 Oxidative stress evaluation, phenolic compound content and photosynthetic pigments*

443 In the present study, main oxidative stress markers, generally considered useful parameters for the
444 evaluation of the toxicity of pollutants (Choudhury et al., 2017), were evaluated. Hydrogen peroxide
445 is a relatively stable ROS induced in plants by many stress conditions. Such as other ROS
446 (superoxide, hydroxyl radicals), H_2O_2 is a key signalling molecule (Mittler, 2002), but when
447 accumulates above a critical level can induce oxidative stress, with oxidation of proteins, lipids and
448 nucleic acids and damage to cellular structures and metabolism (Parida and Das, 2005). Membrane
449 lipid peroxidation can occur with increased content of malondialdehyde, estimated measuring
450 TBARS concentration, considered for this reason a useful parameter, indirect indicator of membrane
451 damage. Under nanoplastic treatments both increase and decrease in oxidative stress parameters have
452 been recorded depending on plant species and/or organ and plastic characteristics (Giorgetti et al.,
453 2020; Li et al., 2020b; Spanò et al., 2022). In our study, both hydrogen peroxide ($F_{2,9}$= 440,8, $p<0.001$)
454 and TBARS ($F_{2,9}$= 219.3, $p<0.001$) contents were significantly higher in *C. nodosa* shoots treated by
455 NPs than in controls and MPs-treated plants (Fig. 3a). Under this latter treatment, H_2O_2 concentration
456 was even lower than in control. Histochemical detection of H_2O_2 by DAB method on isolated leaves
457 showed the highest staining intensity in NPs-treated plants, both in leaf tip and in mid-leaf portions,
458 followed by a less stainability with MPs treatment and even less in the controls (Fig. 4a-f). TBARS
459 content was significantly higher in treated plants (Fig. 3c), especially in NPs samples, than in control,
460 following the same trend recorded in isolated leaves for *in situ* TBARS localization by Schiff's
461 reagent (Fig. 4g-l). In rhizome, H_2O_2 content was significantly lower in NPs-treated plants ($F_{2,9}$=
462 17.35, $p<0.001$), in which oxidative damage (in terms of TBARS) reached however the highest value
463 ($F_{2,9}$= 78.94, $p<0.001$; (Fig. 3b). As under this treatment NPs have been detected inside the plants, a
464 direct membrane damage by these particles, not completely H_2O_2-dependent, could be hypothesized.
465 MPs plants showed intermediate values of TBARS between control and NPs plants (Fig. 3d).
466 Histochemical analysis for H_2O_2 in rhizome by Amplex probe staining displayed a different

467 localization pattern between the control and the treated samples, the latter with a preferential more
468 intense staining in the outer cortical tissues respect to the control (Fig. 5a-c). This peculiar staining
469 pattern indicates that the more peripheral tissues of the rhizome are more sensitive to treatments. The
470 physico-chemical interaction of plastics with the first barriers of the plant cell/tissues can cause
471 distortions and alterations in cell wall structure and functioning, such as to cause unbalanced cellular
472 responses and damage to the plant physiology independently to their uptake, which is generally
473 hampered in case of high molecular weight and large size particles (Kumari et al., 2022).

474 Bodipy probe staining is a histochemical method giving us an outline on membrane damage and
475 allowing to appraise *in situ* lipid peroxidation. The analysis of *C. nodosa* rhizome cross sections
476 showed preferential green signal localized in the epidermis and in the vascular bundles in control
477 samples (Fig. 5d); the same pattern but with higher staining intensity was recorded following plastic
478 treatments (Fig. 5e-f), particularly for NPs samples (Fig. 5f). Similarly to what was underlined for
479 H_2O_2, these differences indicated that the epidermis was particularly responsive to the treatments,
480 being in contact with growth matrix and with both plastics materials. Particles made of PS can directly
481 affect epidermis cell membranes, while for vascular bundles, the localized tissue-specific membrane
482 damages may be the result of a stress-induced cascade of cyto-physiological responses both uptake
483 and non-uptake dependent.

484 In response to oxidative stress, plants have evolved a complex antioxidant machinery, both
485 enzymatic and non-enzymatic, able to counteract the harmful effects of ROS. Phenols are important
486 protective components of plant cells, being able to act as antioxidants due to their capacity to work
487 as hydrogen donors, reducing agents, and singlet O_2 quenchers (Rice-Evans et al., 1997). Phenol
488 content was considerably higher (4-5 folds) in *C. nodosa* rhizome (Fig. 3f) than in shoot (Fig. 3e). In
489 shoot, treatments induced higher contents of these antioxidant molecules and the highest value was
490 observed with NPs-treated plants ($F_{2,9}$= 187.1, $p<0.001$), characterized however by the highest
491 concentration of hydrogen peroxide. In rhizome, only under MPs treatment there was a higher phenol
492 value than in control and NPs plants ($F_{2,9}$= 13.61, $p<0.005$). Pigment content was basically higher in

treated plants, but values of both total chlorophyll (Fig. 6a) and carotenoid (Fig. 6b) content were significantly higher than in control only with MPs ($F_{2,9}$= 7.5, $p<0.05$ and $F_{2,9}$= 18.89, $p<0.01$, respectively). Neither Chla/Chlb ratio nor Carotenoid/total Chl ratio differed significantly among plants (data not shown). The relatively high contents of phenols and photosynthetic pigments in treated plants suggest a good ability of *C. nodosa* to deal with the restrictive conditions induced by MP/NPs. Adventitious roots tended to slough off and degenerate (data not shown) precluding their morpho-anatomical and histochemical analyses.

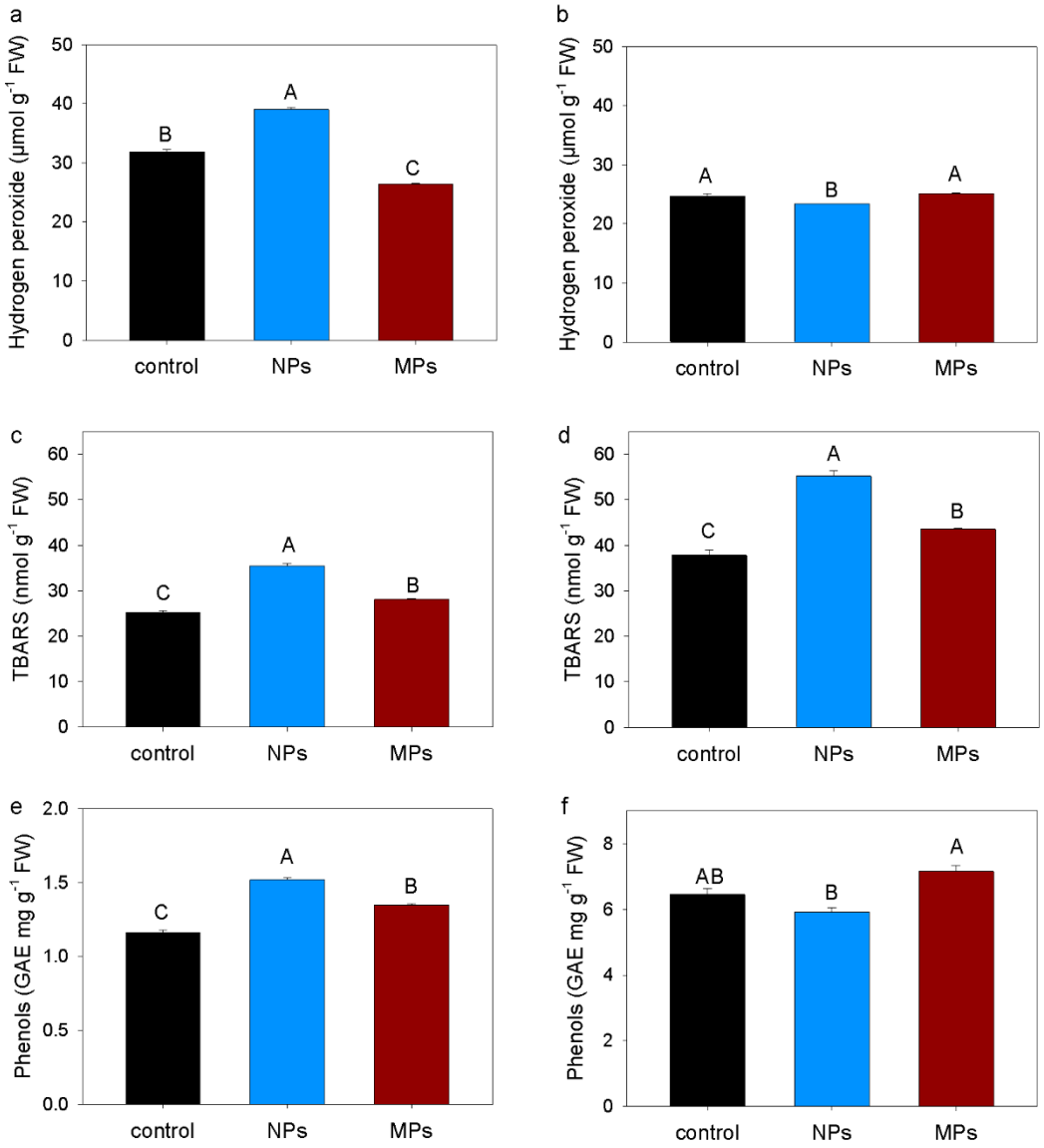

Fig. 3 Concentration of (a,b) hydrogen peroxide, (c,d) thiobarbituric acid reactive substances (TBARS), and (e,f) phenols in shoot (left panels) and rhizome (right panels) of *Cymodocea nodosa* plants grown in control conditions (control, without plastic polystyrene particles) or treated by NPs

or MPs. Different letters above bars denote significant differences ($p < 0.05$) among treatments. Values are means ± SE, n = 4.

1.5 column fitting image, color in online version only

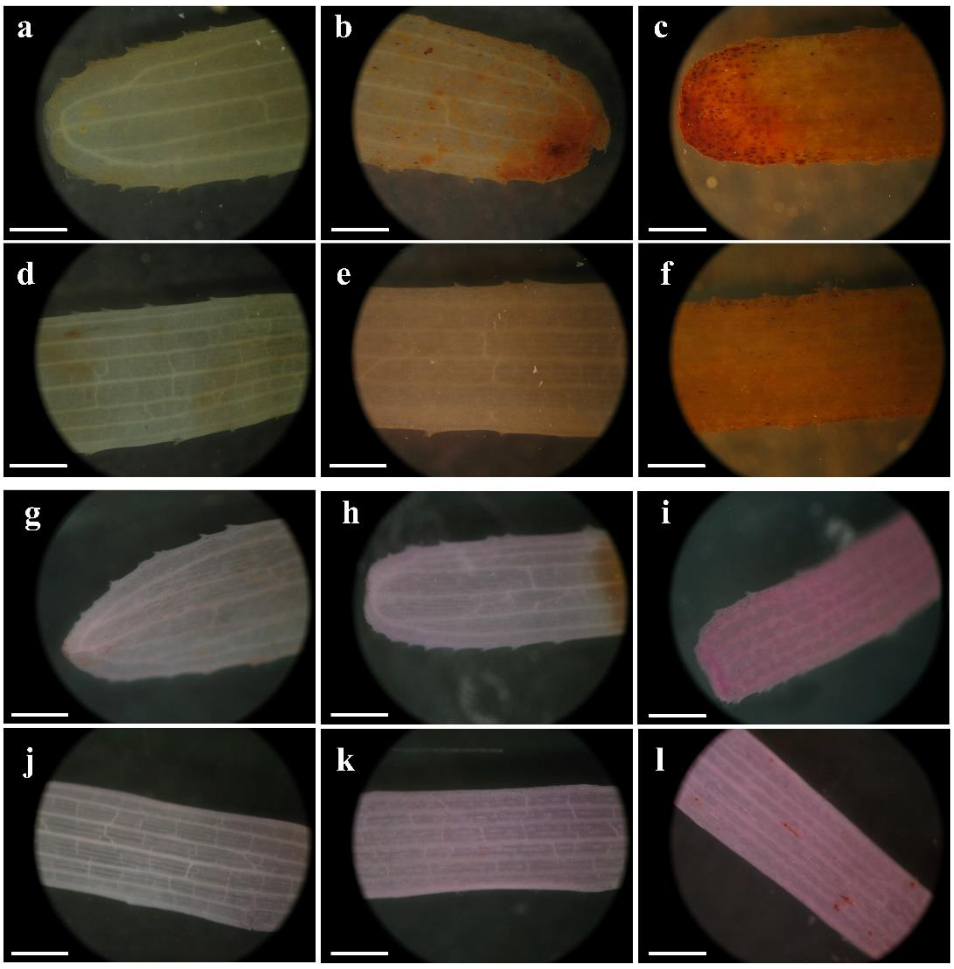

Fig. 4 Representative images of leaf portions of *Cymodocea nodosa* plants processed to histochemical detection of oxidative stress markers. (a-f) DAB staining (H_2O_2 indicator), (g-l) Schiff's reagent staining (lipid peroxidation indicator). a, d and g, j: leaf tip and mid-leaf portion from control sample; b, e and h, k leaf tip and mid-leaf portion from MPs treated plant; c, f and i, l: leaf tip and mid-leaf portion from NPs treated plants. Scale bar = 1 mm.

1.5 column fitting image, color in online version only

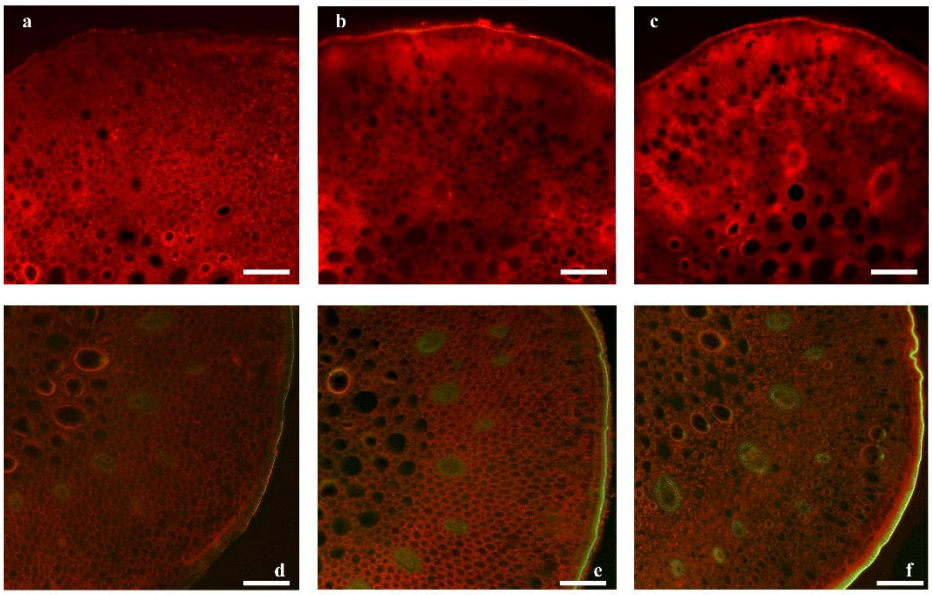

Fig. 5 Representative images of rhizome cross sections of *Cymodocea nodosa* plants processed to histochemical detection of oxidative stress markers. (a-c) staining with Amplex probe (H_2O_2 indicator), (d-f) staining with Bodipy probe (lipid peroxidation indicator). a,d = Control samples; b, e = MPs treated samples; c, f = NPs treated sample. Scale bar = 100 μm.

1.5 column fitting image, color in online version only

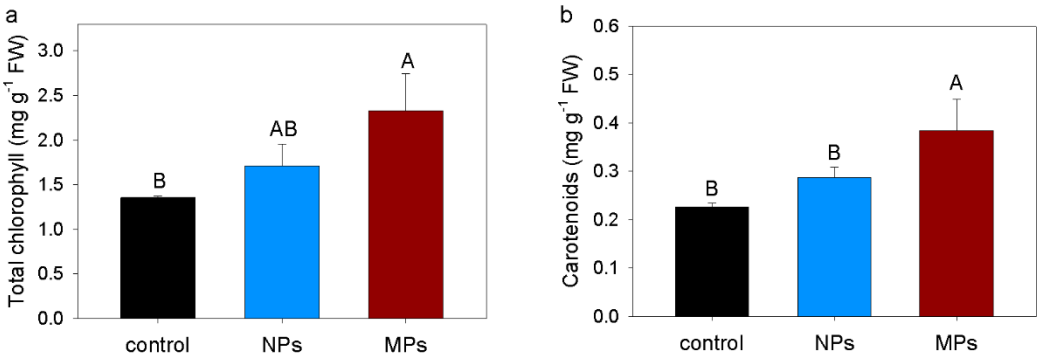

Fig. 6 Concentration of (a) total chlorophyll and (b) carotenoids in leaves of *Cymodocea nodosa* plants grown without plastic polystyrene particles (control) or treated by NPs or MPs. Different letters above bars denote significant differences ($p < 0.05$) among treatments. Values are means ± SE., n =4.

1.5 column fitting image, color in online version only

3.4 Photosynthetic efficiency

571 The JIP test (Tsimilli-Michael, 2020) demonstrated that the effects of PS treatments on *C. nodosa*
572 plants changed depending on the size of particles and the time of exposure. Figure 7a-f report only
573 those parameters that were significantly different from the control ($p < 0.05$), either in NPs- or in
574 MPs-treated plants. Data recorded at day 0 were omitted, because there was not any significant
575 difference between control and treated plants.

576 Exposing plants to MPs for 2 days caused extensive negative effects on photochemical efficiency
577 of plants, whereas NPs did not have any significant impact. The JIP test showed that four groups of
578 parameters varied in the presence of MPs. The first group was that of the technical parameters (Fig.
579 7a). These show that MPs induced a decrease of the amount of the PSII primary acceptor QA, as
580 demonstrated by the lower Area compared to the Control ($\chi^2 = 6.813$; df = 2). This treatment seemed
581 to increase the number of electron transporters per reaction center (RC), as suggested by the greater
582 value of Sm in MPs plants ($\chi^2 = 6.813$; df = 2) and this in turn led to a longer time to achieve the
583 maximum fluorescence emission, as indicated by the higher t for Fm ($\chi^2 = 6.711$; df = 2).
584 Nevertheless, it should be borne in mind that the higher Sm reveals only an apparent increase of the
585 number of electron transporters per RC, which could be simply the consequence of the decreased
586 number of QA acceptors: in other terms, the lower the number of primary electron acceptors, the
587 lower the flow of energy through the transport chain. The decrease of QA acceptors lowered the
588 efficiency of photonic energy input into the primary photochemical event (as displayed by the lower
589 Fv/Fm of MPs plants) ($\chi^2 = 7.378$; df = 2). Also, the donor side of PSII was negatively affected by
590 MPs, that reduced the efficiency of the Hill reaction (lower Fv/Fo compared to the control) ($\chi^2 =$
591 6.436; df = 2); nevertheless, the oxygen evolving complex did not seem to be damaged, as indicated
592 by the low values of Vk ($\chi^2 = 6.813$; df = 2) and dV/dto ($\chi^2 = 8.195$; df = 2). Moreover, despite these
593 negative effects, apparently there was not a rapid accumulation of closed RCs in MPs plants, because
594 Vj was low ($\chi^2 = 8.195$; df = 2). These conflicting data are not simple to interpret, but it may be
595 hypothesised that the negative effects of MPs could have been mitigated by a high connectivity, which
596 is proven by the lower value of dVG/dto in the treated plants, respect to the control ($\chi^2 = 9.262$; df =

2). The enhanced connectivity between antenna complexes of different RCs might have facilitated the transfer of excitation energy between antennas, thus effectively redistributing such energy to those RCs that were open at a given time. Connectivity may consist also in the direct spillover of the excitation energy from PSII to PSI, which might have effectively contributed to reopen PSII RCs (Krüger et al., 2014). Exposure to low photosynthetic photon flux density (PPFD) is known to increase connectivity (Ceusters et al., 2019): it could be speculated that MPs might have shaded leaves, thus inducing the observed phenomenon.

Following 2 days of exposure to MPs, a further group of parameters, i.e., specific energy fluxes per active RC (of PSII), underwent significant changes. The treatment weakened the flux of energy over a wide part of the electron transport chains fed by active RCs (Fig. 7b). The JIP test highlighted the decline of photon absorption (ABS/RC) (χ^2 = 8.195; df = 2), absorbed photon energy trapping (TRo/RC) (χ^2 = 8.697; df = 2) and energy input into the transport chain (ETo/RC) (χ^2 = 6.625; df = 2). The lower energy dissipation per active RC (DIo/RC) (χ^2 = 7.378; df = 2) might have been the consequence of the diminished absorption of photons (ABS/RC). Only the section of the electron transport chain from plastocyanin to the end acceptors did not exhibit a lower performance, but the overall outcome of the treatment with MPs was a loss of efficiency of energy absorption and transport per active RC.

The parameters of the group encompassing efficiencies and quantum yields provide a measure of the ratios between energy fluxes. Efficiencies express the proportion of energy transferred through any single step along the photosynthetic energy flux, therefore they quantify the efficiency of each step of the process. Quantum yields measure the proportion of energy, per absorbed photon, transferred through a given series of steps of the photosynthetic energy flux, i.e., they express the efficiency of energy transport from photon absorption to the selected step. Fig. 7c shows that MPs affected both negatively and positively some of the parameters belonging to this group. The quantum yield of primary photochemistry (φ(Po), equivalent to the afore mentioned Fv/Fm) was lessened by these particles (χ^2 = 6.436; df = 2), which means that a lower amount of photon energy was trapped

623 into the primary acceptor QA: in other terms, the treatment reduced the efficiency of the process that
624 transforms light into chemical energy. Positive effects were exhibited by the efficiency of energy
625 transfer from QA to QB and to the transporters further ahead, on the donor side of PSI (ψ(Eo)) (χ^2 =
626 8.195; df = 2) and by the quantum yield of the related process (φ(Eo)) (χ^2 = 8.195; df = 2), i.e., the
627 proportion of absorbed photon energy that reached plastocyanin. This seems to contradict what has
628 been discussed previously, namely that MPs reduced the energy input into the transport chain per
629 active RC (i.e., lower ETo/RC). This apparent discrepancy may be explained by considering that
630 ETo/RC is a measure of the energy flow, per active RC, through the intersystem electron transporters,
631 while ψ(Eo) is the proportion of energy, per single electron transported, transferred from QA to
632 plastocyanin and φ(Eo) is the proportion of energy, per single photon absorbed, transferred from the
633 antenna complexes to plastocyanin. On this basis, it can be suggested that MPs weakened the flow of
634 energy that each active RC conveyed to the associated electron transport chain, even though such
635 energy was transferred efficiently, at least until plastocyanin.
636 The fourth group of parameters that were significantly affected by MPs encompasses the
637 phenomenological energy fluxes per analysed leaf cross section. These provide a measurement of the
638 energy flow that is occurring within the leaf. They are identified by the notation “o” when calculated
639 on the basis of the fluorescence signal recorded at T = 0 (i.e., upon switching on the light and starting
640 data acquisition, when all RCs are open), or “m” when referred to T = 1 s (i.e., at maximum
641 fluorescence emission by the leaf, when all RCs are closed) (Krüger et al., 2014). Fig. 7d illustrates
642 that MPs had a remarkable negative effect on *C. nodosa* photosynthetic machinery, both at T = 0 and
643 at T = 1 s. The applied particles strongly decreased photon absorption by antenna complexes
644 (ABS/CS) (χ^2 = 7.378 and χ^2 = 7.233 at T = 0 and T = 1, respectively; df = 2), the number of active
645 RCs (RC/CS) (χ^2 = 6.499 and χ^2 = 7.064 at T = 0 and T = 1, respectively; df = 2), photon energy
646 trapping into the primary acceptor QA (TRo/CS) (χ^2 = 7.755 and χ^2 = 7.064 at T = 0 and T = 1,
647 respectively; df = 2), energy transfer from quinone QA to plastocyanin (ETo/CS) (χ^2 = 6.436 both at
648 T = 0 and T = 1; df = 2) and energy transfer from plastocyanin to the final transporters of the chain,

649 on the acceptor side of PSI (REo/CS) (χ^2 = 7.378 and χ^2 = 8.195 at T = 0 and T = 1, respectively; df
650 = 2). Given the lower absorption of photons, also the dissipation of absorbed energy declined
651 (DIo/CS) (χ^2 = 6.813 and χ^2 = 7.378 at T = 0 and T = 1, respectively; df = 2). Overall, this set of
652 parameters demonstrated that, 2 days after treatment, MPs actually impaired the energy processing
653 of all the light reactions of photosynthesis.

654 At the end of the treatment period, NPs did not show any significant effect, while those of MPs
655 were extremely weak. The latter particles lowered the overall quantum yield of energy flow along the
656 transport chain, up to the acceptor side of PSI (φ(Ro)) (χ^2 = 5.645; df = 2) (Fig. 7e). Despite this, no
657 serious negative consequences on photosynthetic light reactions were detected at whole leaf level.
658 The treatment with MPs increased the proportion of dissipated energy when all RCs are open
659 (DIo/CSo) (χ^2 = 6.436; df = 2) (Fig. 7f), which might be the cause of the observed reduction of φ
660 (Ro). Thus, 12 days after the treatment with MPs, plants seemed to have almost completely recovered
661 from the detrimental effects observed at day 2.

662 As previously mentioned (see paragraph 3.1), MPs may stick to the leaf surface and in this way
663 they might have restricted light interception by photosynthetic pigments. This might explain the
664 different effects observed for NPs, that showed the ability of crossing cell membranes, thus
665 penetrating more in depth into the leaves (see paragraph 3.1). Light shortage by MPs is suggested by
666 some parameters of the JIP test performed at day 2, namely ABS/RC, ABS/CSo and ABS/CSm.
667 The lower PPFD might be responsible also for the higher chlorophyll concentration recorded at day
668 12 in MPs-treated plants since an increased amount of the pigment is a well-known feature of the
669 acclimation to a lower radiation. This response, along with other compensatory changes, might have
670 contributed to successfully restoring the photochemical efficiency of MPs plants at day 12, as
671 suggested by the results of the JIP test at that time. These revealed only a slight decline of the general
672 performance of the light reactions, probably attributable to an increased dissipation of the photon
673 energy absorbed: it is worth noting that this process might have been enhanced by the increased
674 concentration of carotenoids in leaves recorded at day 12, as these molecules are key players of the

dissipation processes. The recovery of *C. nodosa* from the negative effects observed at day 2 confirms its ability to acclimate to the shading as previously observed by Malta et al. (2006) and Silva et al. (2013).

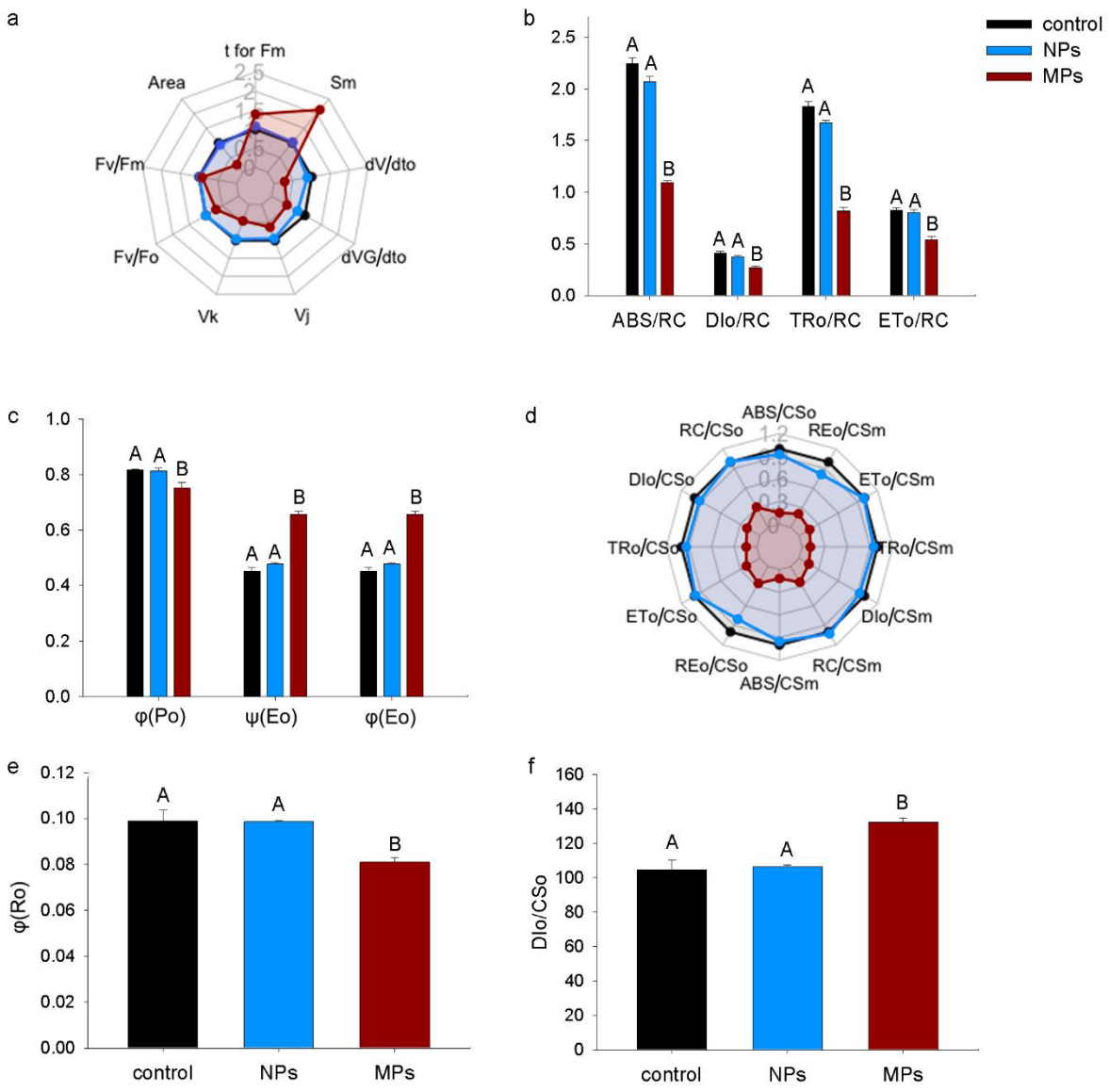

Fig. 7 Results of the JIP test performed at day 2 (a, b, c, d) and day 12 (e, f) on *Cymodocea nodosa* leaves. Only the groups of parameters exhibiting significant differences between control and treated plants are shown. Technical parameters are reported in panel a, specific energy fluxes per active RC in panel b, efficiencies and quantum yields in panels c and e, and phenomenological energy fluxes per analysed leaf cross section in panels d and f. Data of NPs and MPs in panels a and d are referred

to the control, that was made = 1. Values are means ± SE, n = 4 (error bars not shown in panels a and d). Different letters in panels b, c, e, f indicate significant differences ($p < 0.05$) between control and treated plants for each parameter. In panels a and d the data of MPs differed significantly from the control, while those of NPs did not.

Two column fitting image, color in online version only

4. Conclusions

This study revealed that a short-term exposure to an environmentally relevant concentration of MP/NPs made of PS had a considerable effect on the growth and physiological status of the seagrass *C. nodosa* promoting root degeneration, leaf loss and inducing oxidative stress. Besides, MPs also impaired plant photosynthetic machinery. MPs effects could be mainly related to their adhesion on the surfaces of leaves, rhizomes, and roots while NPs effects could be due to their internalization. The increased production of phenolic compounds and photosynthetic pigments and the recovery of photosynthetic efficiency observed after 12 days of exposure indicate that the study species could survive to PS MP/NP exposure on short-term. However, on long-term the exposure to these pollutants could lead to shoot decline and thinning of meadows. This ultimately could translate in a reduction of seagrass ecosystem services, such as water column oxygenation, water flow attenuation, and support to various stages in the life cycles of other organisms. Moreover, the grazing of polluted plants would represent a new, still overlooked entry route of PS NPs in the marine food web. Overall, this study provides new valuable insights into the impact of MP/NPs on marine organisms and underlines the importance of preventing a further introduction of plastic debris in natural environments. It also highlights the need of a systematic monitoring of seagrass meadows as well as of studies aimed at evaluating the actual risks associated to MP/NPs for the health of marine ecosystems.

Statement of Environmental Implication (max 100 words)

This study investigates the effects of an environmentally relevant concentration of two kinds of pollutants of emerging concern, micro- and nanoplastics, on seagrasses which are important habitat-former species at the bottom of marine food webs. Polystyrene micro- and nanoplastics adversely affected seagrass growth by severely damaging roots and increasing leaf loss, and they induced oxidative stress. Besides, microplastics impaired seagrass photosynthetic machinery. Our findings provide the first experimental evidence of the potential risks of prolonged exposure to micro(nanoplastics) for seagrass ecosystems. They can also help in developing targeted measures to protect seagrass habitats from plastic pollution.

CRediT author statement

Virginia Menicagli: Methodology, Formal analysis, Investigation (plant sampling, plant cultivation, plant growth measurements), Visualization, Writing - Review & Editing. **Monica Ruffini Castiglione:** Methodology, Formal analysis, Investigation (SEM analyses of particles and plants), Visualization, Writing - Review & Editing, Supervision, Funding acquisition. **Elena Balestri:** Conceptualization, Methodology, Formal analysis, Investigation (plant sampling, plant cultivation, plant growth measurements), Visualization, Supervision, Writing - Review & Editing. **Lucia Giorgetti:** Methodology, Formal analysis, Investigation (SEM analyses of particles and plants), Visualization, Writing - Review & Editing. **Stefania Bottega:** Methodology, Formal analysis, Investigation (SEM analyses of particles), Visualization, Writing - Review & Editing. **Carlo Sorce:** Methodology, Formal analysis, Investigation (photosynthetic efficiency measurements), Visualization, Writing - Review & Editing. **Carmelina Spanò:** Methodology, Formal analysis, Investigation (oxidative stress evaluation, phenolic compound content and photosynthetic pigments measurements), Visualization, Writing - Review & Editing, Funding acquisition. **Claudio Lardicci:** Methodology, Formal analysis, Investigation (plant sampling, plant cultivation, plant growth measurements), Writing - Review & Editing, Supervision, Funding acquisition.

Declaration of competing interest

The authors declare that they have no known competing financial interests or personal relationships that could have appeared to influence the work reported in this paper.

Funding

This work was supported by University of Pisa, Italy (*Fondi di Ateneo*, FA, and *Progetti di Ricerca di Ateneo*, PRA). The funding sources had no role in study design, in the collection, analysis and interpretation of data.

References

Adamakis, I.-D.S., Malea, P., Panteris, E., 2018. The effects of Bisphenol A on the seagrass *Cymodocea nodosa*: Leaf elongation impairment and cytoskeleton disturbance. Ecotoxicol. Environ. Saf. 157, 431-440. https://doi.org/10.1016/j.ecoenv.2018.04.005

Andrady, A.L., 2011. Microplastics in the marine environment. Mar. Pollut. Bull. 62, 1596–1605. https://doi.org/10.1016/j.marpolbul.2011.05.030

Arezki, O., Boxus, P., Kevers, C., Gaspar, T., 2001. Changes in peroxidase activity, and level of phenolic compounds during light-induced plantlet regeneration from *Eucalyptus camaldulensis* Dehn. nodes in vitro. Plant Growth Regul. 33, 215–219. https://doi.org/10.1023/A:1017579623170

ARPAT, 2014. Direttiva 2000/60/CE Qualità delle acque marino costiere prospicienti lo scarico Solvay di Rosignano.

Balestri, E., Menicagli, V., Vallerini, F., Lardicci, C., 2017. Biodegradable plastic bags on the seafloor: A future threat for seagrass meadows? Sci. Total Environ. 605-606, 755-763. http://dx.doi.org/10.1016/j.scitotenv.2017.06.249

Balestri, E., Vallerini, F., Seggiani, M., Cinelli, P., Menicagli, V., Vannini, C., Lardicci, C., 2019. Use of bio-containers from seagrass wrack with nursery planting to improve the eco-

779 sustainability of coastal habitat restoration. J. Env. Manag. 251, 109604.
780 https://doi.org/10.1016/j.jenvman.2019.109604
781 Barbier, E.B., Hacker, S.D., Kennedy, C., Koch, E.W., Stier, A.C., Silliman, B.R., 2011. The value
782 of estuarine and coastal ecosystem services. Ecol. Monogr. 81, 169-193.
783 https://doi.org/10.1890/10-1510.1
784 Beiras, R., Schönemann, A.M., 2020. Currently monitored microplastics pose negligible ecological
785 risk to the global ocean. Sci. Rep. 10, 22281. https://doi.org/10.1038/s41598-020-79304-z
786 Bergami, E., Pugnalini, S., Vannuccini, M.L., Manfra, L., Faleri, C., Savorelli, F., Dawson, K.A.,
787 Corsi, I., 2017. Long-term toxicity of surface-charged polystyrene nanoplastics to marine
788 planktonic species *Dunaliella tertiolecta* and *Artemia franciscana.* Aquat. Toxicol. 189, 159-
789 169. http://dx.doi.org/10.1016/j.aquatox.2017.06.008
790 Bergmann, M., Gutow, L., Klages, M., 2015. Marine Anthropogenic Litter. SpringerOpen.
791 Besseling, E., Wang, B., Lürling, M., Koelmans, A.A., 2014. Nanoplastic affects growth of *S.*
792 *obliquus* and reproduction of *D. magna*. Environ. Sci. Technol. 48, 12336–12343.
793 https://doi.org/10.1021/es503001d
794 Besseling, E., Redondo-Hasselerharm, P., Foekema, E.M., Koelmans, A.A., 2019. Quantifying
795 ecological risks of aquatic micro-and nanoplastic. Crit. Rev. Env. Sci. Tec. 49, 32–80.
796 https://doi.org/10.1080/10643389.2018.1531688
797 Blair, R. M., Waldron, S., Phoenix, V., Gauchotte-Lindsay, C., 2017. Micro and nanoplastic
798 pollution of freshwater and wastewater treatment systems. Springer Sci. Rev. 5, 19–30.
799 https://doi.org/10.1007/s40362-017-0044-7
800 Bhattacharya, P., Lin, S., Turner, J.P., Ke, P.C., 2010. Physical adsorption of charged plastic
801 nanoparticles affects algal photosynthesis. J. Phys. Chem. C. 114, 16556–16561.
802 https://doi.org/10.1021/jp1054759

803 Boots, B., Russell, C.W., Green, D.S., 2019. Effects of microplastics in soil ecosystems: Above and
804 below ground. Environ. Sci. Technol. 53, 19, 11496–11506.
805 https://doi.org/10.1021/acs.est.9b03304
806 Bosker, T., Bouwman, L.J., Brun, N.R., Behrens, P., Vijver, M.G., 2019. Microplastics accumulate
807 on pores in seed capsule and delay germination and root growth of the terrestrial vascular plant
808 *Lepidium sativum*. Chemosphere 226, 774–781.
809 https://doi.org/10.1016/j.chemosphere.2019.03.163
810 Cabaço, S., Ferreira, O., Santos, R., 2010. Population dynamics of the seagrass *Cymodocea nodosa*
811 in Ria Formosa lagoon following inlet artificial relocation. Estuar. Coast Shelf. Sci. 87, 510–516.
812 https://doi.org/10.1016/j.ecss.2010.02.002
813 Cao, J., Liao, Y., Yang, W., Jiang, X., Li, J.M., 2022. Enhanced microalgal toxicity due to
814 polystyrene nanoplastics and cadmium co-exposure: From the perspective of physiological and
815 metabolomic profiles. J. Hazard. Mat., 427, 127937.
816 https://doi.org/10.1016/j.jhazmat.2021.127937
817 Capolupo, M., Sørensen, L., Jayasena, K.D.R., Booth, A.M., Fabbri, E., 2020. Chemical
818 composition and ecotoxicity of plastic and car tire rubber leachates to aquatic organisms. Water
819 Res. 169, 115270. https://doi.org/10.1016/j.watres.2019.115270
820 Cauwenberghe, L.V., Devriese, L., Galgani, F., Robbens, J., Janssen, C.R., 2015. Microplastics in
821 sediment: a review of techniques, occurrence and effects. Mar. Environ. Res., 111, 5-17.
822 https://doi.org/10.1016/j.marenvres.2015.06.007
823 Ceusters, N., Valcke, R., Frans, M., Claes, J.E., Van den Ende, W., Ceusters, J., 2019. Performance
824 index and PSII connectivity under drought and contrasting light regimes in the CAM orchid
825 *Phalaenopsis*. Front. Plant Sci. 10, 1012. https://doi.org/10.3389/fpls.2019.01012
826 Chae, Y., An, Y.-J., 2017. Effects of micro- and nanoplastics on aquatic ecosystems: Current
827 research trends and perspectives. Mar. Pollut. Bull. 124, 624-632.
828 http://dx.doi.org/10.1016/j.marpolbul.2017.01.070

829 Choudhury, F.K., Rivero, R.M., Blumwald, E., Mittler, R., 2017. Reactive oxygen species, abiotic
830 stress and stress combination. Plant J. 90, 856–867. https://doi.org/10.1111/tpj.13299
831 Corsi, I., Bergami, E., Grassi, G., 2020. Behavior and bio-interactions of anthropogenic particles in
832 marine environment for a more realistic ecological risk assessment. Front. Environ. Sci. 8, 60.
833 https://doi.org/10.3389/fenvs.2020.00060
834 Cozzolino, L., Nicastro, K.R., Zardi, G.I., de los Santos, C.B., 2020. Species-specific plastic
835 accumulation in the sediment and canopy of coastal vegetated habitats. Sci. Total Environ. 723,
836 138018. https://doi.org/10.1016/j.scitotenv.2020.138018
837 Cunha, A.H., Duarte, C.M., 2007. Biomass and leaf dynamics of *Cymodocea nodosa* in the Ria
838 Formosa lagoon, South Portugal. Bot. Mar. 50, 1-7. https://doi.org/10.1515/BOT.2007.001
839 da Costa, J.P., Santos, P.S.M., Duarte, A.C., Rocha-Santos, T., 2016. (Nano)plastics in the
840 environment – Sources, fates and effects. Sci. Total Environ. 566-567, 15-26.
841 http://dx.doi.org/10.1016/j.scitotenv.2016.05.041
842 Dahl, M., Bergman, S., Björk, M., Diaz-Almela, E., Granberg, M., Gullström, M., Leiva-Dueñas,
843 C., Magnusson, K., Marco-Méndez, C., Piñeiro-Juncal, N., Mateo, M.A., 2021. A temporal
844 record of microplastic pollution in Mediterranean seagrass soils. Environ. Pollut. 273, 116451.
845 https://doi.org/10.1016/j.envpol.2021.116451
846 Daudi, A., O'Brien, J.A., 2012. Detection of hydrogen peroxide by DAB staining in *Arabidopsis*
847 leaves. Bio Protoc. 2(18): e263.
848 De los Santos, C., Krang, A., Infantes, E., 2021. Microplastic retention by marine vegetated
849 canopies: Simulations with seagrass meadows in a hydraulic flume. Environ. Pollut., 269,
850 116050. https://doi.org/10.1016/j.envpol.2020.116050
851 Dovidat, L.C., Brinkmann, B.W., Vijver, M.G., Bosker, T., 2019. Plastic particles adsorb to the
852 roots of freshwater vascular plant *Spirodela polyrhiza* but do not impair growth. L&O Letters 5,
853 37-45. https://doi.org/10.1002/lol2.10118

854 Duarte, C.M., Sand-Jensen, K., 1990. Seagrass colonization: Patch formation and patch growth in
855 *Cymodocea nodosa*. Mar. Ecol. Progr. Ser. 65, 193-200. https://doi.org/10.3354/meps065193
856 Eriksen, M., Lebreton, L.C.M., Carson, H.S., Thiel, M., Moore, C.J., Borerro, J.C., Galgani, F.,
857 Ryan, P.G., Reisser, J., 2014. Plastic pollution in the world's oceans: More than 5 trillion plastic
858 pieces weighing over 250,000 tons afloat at sea. Plos ONE 9(12), e111913.
859 https://doi.org/10.1371/journal.pone.0111913
860 Ferreira, I., Venâncio, C., Lopes, I., Oliveira, M., 2019. Nanoplastics and marine organisms: What
861 has been studied? Environ. Toxicol. Pharmacol. 67, 1-7.
862 https://doi.org/10.1016/j.etap.2019.01.006
863 Gangadoo, S., Owen, S., Rajapaksha, P., Plaisted, K., Cheeseman, S., Haddar, H., Khanh Truong,
864 V., Ngo, S.T., Vu, V.V., Cozzolino, D., Elbourne, A., Crawford, R., Lathama, K., Chapman, J.,
865 2020. Nano-plastics and their analytical characterisation and fate in the marine environment:
866 From source to sea. Sci. Total Environ. 732, 138792.
867 https://doi.org/10.1016/j.scitotenv.2020.138792
868 Gao, G., Zhao, X., Jin, P., Gao, K., Beardall, J., 2021. Current understanding and challenges for
869 aquatic primary producers in a world with rising micro- and nanoplastic levels. J. Hazard. Mater.
870 406, 124685. https://doi.org/10.1016/j.jhazmat.2020.124685
871 Garrido, S., Linares, M., Campillo, J.M., Albentosa, M., 2019. Effect of microplastics on the
872 toxicity of chlorpyrifos to the microalgae *Isochrysis galbana*, clone t-ISO. Ecotoxicol. Environ.
873 Saf. 173, 103-109. https://doi.org/10.1016/j.ecoenv.2019.02.020
874 Gerstenbacher, C.M., Finzi, A.C., Rotjan, R.D., Novak, A.B., 2022. A review of microplastic
875 impacts on seagrasses, epiphytes, and associated sediment communities. Environ. Pollut. In
876 Press, 119108. https://doi.org/10.1016/j.envpol.2022.119108
877 Giorgetti, L., Spanò, C., Muccifora, S., Bottega, S., Barbieri, F., Bellani, L., Castiglione, M.R.,
878 2020. Exploring the interaction between polystyrene nanoplastics and *Allium cepa* during

germination: internalization in root cells, induction of toxicity and oxidative stress. Plant Physiol. Biochem. 149, 170–177. https://doi.org/10.1016/j.plaphy.2020.02.014

Giorgetti, L., Spanò, C., Muccifora, S., Bellani, L., Tassi, E., Bottega, S., Di Gregorio, S., Siracusa, G., Sanità di Toppi, L., Ruffini Castiglione, M., 2019. An integrated approach to highlight biological responses of *Pisum sativum* root to nano-TiO_2 exposure in a biosolid-amended agricultural soil. Sc. Total Env. 650, 2705-2716. https://doi.org/10.1016/j.scitotenv.2018.10.032

Gonçalves, J.M., Bebianno, M.J., 2021. Nanoplastics impact on marine biota: A review. Environ. Pollut. 273, 116426. https://doi.org/10.1016/j.envpol.2021.116426

Goss, H., Jaskiel, J., Rotjan, R., 2018. *Thalassia testudinum* as a potential vector for incorporating microplastics into benthic marine food webs. Mar. Pollut. Bull. 135, 1085-1089. https://doi.org/10.1016/j.marpolbul.2018.08.024

Hartmann, N.B., Hüffer, T., Thompson, R.C., Hassellöv, M., Verschoor, A., Daugaard, A.E., Rist, S., Karlsson, T., Brennholt, N., Cole, M., Herrling, M.P., Hess, M.C., Ivleva, N.P., Lusher, A.L., Wagner, M., 2019. Are we speaking the same language? Recommendations for a definition and categorization framework for plastic debris. Environ. Sci. Technol. 53, 1039-1047. https://doi.org/10.1021/acs.est.8b05297

He, Q., Silliman, B.R., 2019. Climate change, human impacts, and coastal ecosystems in the Anthropocene. Current Biol. 29, R1021-R1035. https://doi.org/10.1016/j.cub.2019.08.042

Huang, Y., Xiao, X., Xu, C., Perianen, Y.D., Hu, J., Holmer, M., 2020. Seagrass beds acting as a trap of microplastics - Emerging hotspot in the coastal region? Environ. Pollut. 257, 113450. https://doi.org/10.1016/j.envpol.2019.113450

Isobe, A., Iwasaki, S., Uchida, K., Tokai, T., 2019. Abundance of non-conservative microplastics in the upper ocean from 1957 to 2066. Nat. Commun. 10, 417. https://doi.org/10.1038/s41467-019-08316-9

Jana, S., Choudhuri, M.A., 1982. Glycolate metabolism of three submerged aquatic angiosperms during aging. Aquat. Bot. 12, 345–354. https://doi.org/10.1016/0304-3770(82)90026-2

905 Jiang, X., Chen, H., Liao, Y., Ye, Z., Li, M., Klobučar, G., 2019. Ecotoxicity and genotoxicity of
906 polystyrene microplastics on higher plant *Vicia faba*. Environ. Pollut. 250, 831-838.
907 https://doi.org/10.1016/j.envpol.2019.04.055
908 Jones, K.L., Hartl, M.G.J., Bell, M.C., Capper, A., 2020. Microplastic accumulation in a *Zostera*
909 *marina* L. bed at Deerness Sound, Orkney, Scotland. Mar. Pollut. Bull. 152, 110883.
910 https://doi.org/10.1016/j.marpolbul.2020.110883
911 Kalaji, H.M., Schansker, G., Ladle, R.J., 2014. Frequently asked questions about in vivo
912 chlorophyll fluorescence: practical issues. Photosynth. Res., 122, 121-158.
913 https://doi.org/10.1007/s11120-014-0024-6
914 Kalčíková, G., Gotvajn, A.Z., Kladnik, A., Jemec, A., 2017. Impact of polyethylene microbeads on
915 the floating freshwater plant duckweed *Lemna minor*. Environ. Pollut. 230, 1108-1115.
916 https://doi.org/10.1016/j.envpol.2017.07.050
917 Koelmans, A.A., Besseling, E., Shim, W.J., 2015. Nanoplastics in the aquatic environment. Critical
918 Review. In: Bergmann, M., Gutow, L., Klages, M. (eds) Marine Anthropogenic Litter. Springer,
919 Cham. https://doi.org/10.1007/978-3-319-16510-3_12
920 Krüger, G.H.J., De Villiers, M.F., Strauss, A.J., de Beer, M., van Heerden, P.D.R., Maldonado, R.,
921 Strasser, R.J., 2014. Inhibition of photosystem II activities in soybean (*Glycine max*) genotypes
922 differing in chilling sensitivity. S. Afr. J. Bot., 95, 85-96.
923 https://doi.org/10.1016/j.sajb.2014.07.010
924 Kumari, A., Rajput, V.D., Mandzhieva, S.S., Rajput, S., Minkina, T., Kaur, R., Sushkova, S.,
925 Kumari, P., Ranjan, A., Kalinitchenko, V.P., Glinushkin, A.P., 2022. Microplastic pollution: an
926 emerging threat to terrestrial plants and insights into its remediation strategies. Plants 11, 340.
927 https://doi.org/10.3390/plants11030340
928 Kuo, J., den Hartog, C., 2006. Seagrass morphology, anatomy, and ultrastructure. In Seagrasses:
929 Biology, Ecology and Conservation, pp. 51–87. A. W. D. Larkum et al. (eds.), Springer.

930 Larue, C., Sarret, G., Castillo-Michel, H., Pradas del Real, A.E., 2021. A critical review on the
931 impacts of nanoplastics and microplastics on aquatic and terrestrial photosynthetic organisms.
932 Small 17, 2005834. https://doi.org/10.1002/smll.202005834
933 Larue, C., Castillo-Michel, H., Sobanska, S., Bureau, S., Barthès, V., Ouerdane, L., Carrière, M.,
934 Sarret, G., 2014. Foliar exposure of the crop *Lactuca sativa* to silver nanoparticles: Evidence for
935 internalization and changes in Ag speciation. J. Hazard. Mater. 261: 98–106.
936 https://doi.org/10.1016/j.jhazmat.2013.10.053
937 Lenz, R., Enders, K., Nielsen, T.G., 2016. Microplastic exposure studies should be environmentally
938 realistic. P. Natl. Acad. Sci. 113, E4121–E4122. https://doi.org/10.1073/pnas.1606615113
939 Leusch, F.D.L., Ziajahromi, S., 2021. Converting mg/L to particles/L: Reconciling the occurrence
940 and toxicity literature on microplastics. Environ. Sci. Technol. 55, 11470−11472.
941 https://doi.org/10.1021/acs.est.1c04093
942 Li, W., Lo, H., Wong, H., Zhou, M., Wong, C., Tam, N.F., Cheung, S., 2020. Heavy metals
943 contamination of sedimentary microplastics in Hong Kong. Mar. Pollut. Bull., 153, 110977.
944 https://doi.org/10.1016/j.marpolbul.2020.110977
945 Li, Z., Li, R., Li, Q., Zhou, J., Wang, G., 2020b. Physiological response of cucumber (*Cucumis*
946 *sativus* L.) leaves to polystyrene nanoplastics pollution. Chemosphere 255, 127041.
947 https://doi.org/10.1016/j.chemosphere.2020.127041
948 Lian, J., Wu, J., Xiong, H., Zeb, A., Yang, T., Su, X., Su, L., Liu W., 2020. Impact of polystyrene
949 nanoplastics (PSNPs) on seed germination and seedling growth of wheat (*Triticum aestivum* L.).
950 J. Hazard. Mat. 385, 121620. https://doi.org/10.1016/j.jhazmat.2019.121620
951 Lian, J., Liu, W., Sun, Y., Men, S., Wu, J., Zeb, A., Yang, T., Ma, L.Q., Zhou, Q., 2022.
952 Nanotoxicological effects and transcriptome mechanisms of wheat (*Triticum aestivum* L.) under
953 stress of polystyrene nanoplastics. J. Hazard. Mat. 423, 127241.
954 https://doi.org/10.1016/j.jhazmat.2021.127241

955 Liu, G., Jiang, R., You, J., Muir, D.C.G., Zeng, E.Y., 2020. Microplastic impacts on microalgae
956 growth: Effects of size and humic acid. Environ. Sci. Technol. 54, 1782−1789.
957 https://doi.org/10.1021/acs.est.9b06187
958 Long, M., Paul-Pont, I., Hégaret, H., Moriceau, B., Lambert, C., Huvet, A., Soudant, P., 2017.
959 Interactions between polystyrene microplastics and marine phytoplankton lead to species-
960 specific hetero-aggregation. Environ. Pollut. 228, 454-463.
961 https://doi.org/10.1016/j.envpol.2017.05.047
962 Luo, H., Xiang, Y., He, D., Li, Y., Zhao, Y., Wang, S., Pan, X., 2019. Leaching behavior of
963 fluorescent additives from microplastics and the toxicity of leachate to *Chlorella vulgaris*. Sci.
964 Total Environ., 678, 1-9. https://doi.org/10.1016/j.scitotenv.2019.04.401
965 Malta, E.J., Brun, F.G., Vergara, J.J., Hernández, I., Pérez-Llorénz, J.L., 2006. Recovery of
966 *Cymodocea nodosa* (Ucria) Ascherson photosynthesis after a four-month dark period. Sci. Mar.
967 70, 413-422. https://doi.org/10.3989/scimar.2006.70n3413
968 Mateos-Cárdenas, A., Scott, D.T., Seitmaganbetova, G., van Pelt, F.N.A.M., O'Halloran, J.,
969 Jansenet, M.A.K., 2019. Polyethylene microplastics adhere to *Lemna minor* (L.), yet have no
970 effects on plant growth or feeding by *Gammarus duebeni* (Lillj.). Sci. Total Environ. 689, 413-
971 421. https://doi.org/10.1016/j.scitotenv.2019.06.359
972 Mateos-Cárdenas, A., van Pelt, F.N.A.M., O'Halloran, J., Jansenet, M.A.K., 2021. Adsorption,
973 uptake and toxicity of micro- and nanoplastics: Effects on terrestrial plants and aquatic
974 macrophytes. Environ. Pollut. 284, 117183. https://doi.org/10.1016/j.envpol.2021.117183
975 Meng, F., Yang, X., Riksen, M., Xu, M., Geissen, V., 2021. Response of common bean (*Phaseolus*
976 *vulgaris* L.) growth to soil contaminated with microplastics. Sci. Total Environ. 755, part
977 2,142516. https://doi.org/10.1016/j.scitotenv.2020.142516
978 Menicagli, V., Balestri, E., Vallerini, F., De Battisti, D., Lardicci, C., 2021. Plastics and
979 sedimentation foster the spread of a non-native macroalga in seagrass meadows. Sci. Total
980 Environ. 757, 143812. https://doi.org/10.1016/j.scitotenv.2020.143812

Mittler, R., 2002. Oxidative stress, antioxidants and stress tolerance. Trends Plant Sci. 7, 405–410. https://doi.org/10.1016/S1360-1385(02)02312-9

Mylona, Z., Panteris, E., Moustakas, M., Kevrekidis, T., Malea, P., 2020a. Physiological, structural and ultrastructural impacts of silver nanoparticles on the seagrass *Cymodocea nodosa*. Chemosphere 248, 126066. https://doi.org/10.1016/j.chemosphere.2020.126066

Mylona, Z., Panteris, E., Kevrekidis, T., Malea, P., 2020b. Effects of titanium dioxide nanoparticles on leaf cell structure and viability, and leaf elongation in the seagrass *Halophila stipulacea*. Sci. Total Environ. 719, 137378. https://doi.org/10.1016/j.scitotenv.2020.137378

Navarrete-Fernández, Bermejo, R., Hernández, I., Deidun, A., Andreu-Cazenave, M., Cózar, A., 2022. The role of seagrass meadows in the coastal trapping of litter. Mar. Pollut. Bull. 174, 113299. https://doi.org/10.1016/j.marpolbul.2021.113299

Orth, R.J., Carruthers, T.J.B., Dennison, W.C., Duarte, C.M., Fourqurean, J.W., Heck, K.L., Hughes, A.R., Kendrick, G.A., Kenworthy, W.J., Olyarnik, S., Short, F.T., Waycott, M., Williams, S.L., 2006. A global crisis for seagrass ecosystems. BioScience 56, 987–996. https://doi.org/10.1641/0006-3568(2006)56[987:AGCFSE]2.0.CO;2

Parida, A.K., Das, A.B., 2005. Salt tolerance and salinity effects on plants: a review. Ecotoxicol. Environ. Saf. 60, 324–349. https://doi.org/10.1016/j.ecoenv.2004.06.010

Pfeifer, L., Classen, B., 2020. The cell wall of seagrasses: fascinating, peculiar and a blank canvas for future research. Front. Plant Sci., 11, 588754. https://doi.org/10.3389/fpls.2020.588754

Qi, Y., Yang, X., Pelaez, A.M., Huerta Lwanga, E., Beriot, N., Gertsen, H., Garbeva, P., Geissen, V., 2018. Macro- and micro- plastics in soil-plant system: effects of plastic mulch film residues on wheat (*Triticum aestivum*) growth. Sci. Total Environ. 645, 1048-1056. https://doi.org/10.1016/j.scitotenv.2018.07.229

Rice-Evans, C.A., Miller, N.J., Pagana, G., 1997. Antioxidant properties of phenolic compounds. Trends Plant Sci. 2, 152-159. https://doi.org/10.1016/S1360-1385(97)01018-2

1006 Ruocco, M., De Luca, P., Marín-Guirao, L., Procaccini, G., 2019. Differential leaf age-dependent
1007 thermal plasticity in the keystone seagrass *Posidonia oceanica*. Front. Plant Sci. 10, 1556.
1008 https://doi.org/10.3389/fpls.2019.01556
1009 Sanchez-Vidal, A., Canals, M., de Haan, W.P., Romero, J., Veny, M., 2021. Seagrasses provide a
1010 novel ecosystem service by trapping marine plastics. Sci. Rep. 11, 254.
1011 https://doi.org/10.1038/s41598-020-79370-3
1012 Sandrini-Neto, L., Camargo, M.G., 2014. GAD: an R package for ANOVA designs from general
1013 principles. R package.
1014 Seeley, M.E., Song, B., Rassir, R., Hale, R.C., 2020. Microplastics affect sedimentary microbial
1015 communities and nitrogen cycling. Nat. Commun., 11, 2372. https://doi.org/10.1038/s41467-
1016 020-16235-3
1017 Seng, N., Lai, S., Fong, J., Saleh, M.F., Cheng, C., Cheok, Z.Y., Todd, P.A., 2020. Early evidence
1018 of microplastics on seagrass and macroalgae. Mar. Freshw. Res. 71, 922-928.
1019 https://doi.org/10.1071/MF19177
1020 Sghaier, Y.R., Zakhama-Sraieb, R., Charfi-Cheikhrouh, F., 2011. Primary production and biomass
1021 in a *Cymodocea nodosa* meadow in the Ghar El Melh lagoon, Tunisia. Bot. Mar. 54, 411-418.
1022 https://doi.org/10.1515/BOT.2011.045
1023 Silva, J., Barrote, I., Costa, M.M., Albano, S., Santos, R., 2013. Physiological responses of *Zostera*
1024 *marina* and *Cymodocea nodosa* to light-limitation stress. PLoS ONE 8, e81058.
1025 https://doi.org/10.1371/journal.pone.0081058
1026 Sjollema, S.B., Redondo-Hasselerharm, P., Leslie, H.A., Kraaka, M.H.S., Vethaak, A.D., 2016. Do
1027 plastic particles affect microalgal photosynthesis and growth? Aquat. Toxicol. 170, 259-261.
1028 http://dx.doi.org/10.1016/j.aquatox.2015.12.002
1029 Spanò, C., Bottega, S., 2016. Durum wheat seedlings in saline conditions: salt spray versus root-
1030 zone salinity. Estuar. Coast Shelf Sci. 169, 173–181. https://doi.org/10.1016/j.ecss.2015.11.031

Spanò, C., Bottega, S., Ruffini Castiglione, M., Pedranzani, H.E., 2017. Antioxidant response to cold stress in two oil plants of the genus *Jatropha*. Plant Soil Environ. 63, 271–276. https://doi.org/10.17221/182/2017-PSE

Spanò, C., Bottega, S., Sorce, C., Bartoli, G., Ruffini Castiglione, M., 2019. TiO_2 nanoparticles may alleviate cadmium toxicity in co-treatment experiments on the model hydrophyte *Azolla filiculoides*. Env. Sc. Poll. Res. 26, 29872-29882. https://doi.org/10.1007/s11356-019-06148-0

Spanò, C., Bottega, S., Bellani, L., Muccifora, S., Sorce, C., Ruffini Castiglione, M., 2020. Effect of Zinc priming on salt response of wheat seedlings: relieving or worsening? Plants 9, 1514. https://doi.org/10.3390/plants9111514

Spanò, C., Muccifora, S., Ruffini Castiglione, M., Bellani, L., Bottega, S., Giorgetti, L., 2022. Polystyrene nanoplastics affect seed germination, cell biology and physiology of rice seedlings in-short term treatments: Evidence of their internalization and translocation. Plant Physiol. Biochem. 172, 158–166. https://doi.org/10.1016/j.plaphy.2022.01.012

Stirbet, A., Lazár, D., Kromdijk, J., Govindjee, 2018. Chlorophyll a fluorescence induction: Can just a one-second measurement be used to quantify abiotic stress responses? Photosynthetica 56, 86-104. https://doi.org/10.1007/s11099-018-0770-3

Sun, X.-D., Yuan, X.-Z., Jia, Y., Feng, L.-J., Zhu, F.-P., Dong, S.-S., Liu, J., Kong, X., Tian, H., 2, Duan, J.-L., Ding, Z., Wang, S.-G., Xing, B., 2020. Differentially charged nanoplastics demonstrate distinct accumulation in Arabidopsis thaliana. Nat. Nanotechnol. 15, 755-760. https://doi.org/10.1038/s41565-020-0707-4

Thompson, R.C., Moore, C.J., vom Saal, F.S., Swan, S.H., 2009. Plastics, the environment and human health: current consensus and future trends. Phil. Trans. R. Soc. B 364, 2153–2166. https://doi.org/10.1098/rstb.2009.0053

Tsimilli-Michael, M., 2020. Revisiting JIP-test: An educative review on concepts, assumptions, approximations, definitions and terminology. Photosynthetica 58, 275-292. https://doi.org/10.32615/ps.2019.150

van Weert, S., Redondo-Hasselerharm, P.E., Diepens, N.J., Koelmanset, A.A., 2019. Effects of nanoplastics and microplastics on the growth of sediment-rooted macrophytes. Sci. Total Environ. 654, 1040-1047. https://doi.org/10.1016/j.scitotenv.2018.11.183

Wang, Y.S., Ding, M.D., Gu, X.G., Wang, J.L., Pang, Y.L., Gao, L.P., Xsia, T., 2013. Analysis of interfering substances in the measurement of malonildialdehyde content in plant leaves. Am. J. Biochem. Biotechnol. 9, 235–242. https://doi.org/10.3844/ajbbsp.2013.235.242

Yamamoto, Y., Yukiko Kobayashi, Y., Matsumoto, H., 2001. Lipid peroxidation is an early symptom triggered by aluminum, but not the primary cause of elongation inhibition in pea roots. Plant Physiol 125, 199–208. https://doi.org/10.1104/pp.125.1.199

Yu, H., Peng, J., Cao, X., Wang, Y., Zhang, Z., Xu, Y., Qi, W., 2021. Effects of microplastics and glyphosate on growth rate, morphological plasticity, photosynthesis, and oxidative stress in the aquatic species *Salvinia cucullate*. Environ. Pollut. 279, 116900. https://doi.org/10.1016/j.envpol.2021.116900

Zhang, C., Chen, X., Wang, J., Tan, L., 2017. Toxic effects of microplastic on marine microalgae *Skeletonema costatum*: Interactions between microplastic and algae. Environ. Pollut. 220, 1282-1288. https://doi.org/10.1016/j.envpol.2016.11.005

Zhao, T., Tan, L., Huang, W., Wang, J., 2019. The interactions between micro polyvinyl chloride (mPVC) and marine dinoflagellate *Karenia mikimotoi*: The inhibition of growth, chlorophyll and photosynthetic efficiency. Environ. Pollut. 247, 883-889. https://doi.org/10.1016/j.envpol.2019.01.114

Zhou, C.-Q., Lu, C.-H., Mai, L., Bao, L.-J., Liu, L.-Y., Zeng, E.Y., 2021. Response of rice (*Oryza sativa* L.) roots to nanoplastic treatment at seedling stage. J. Hazard. Mat. 401, 123412. https://doi.org/10.1016/j.jhazmat.2020.123412

Supplementary material for

"Polystyrene micro- and nanoplastics induce growth and physiological alterations in marine plants (seagrasses)"

Virginia Menicagli[1,2†], Monica Ruffini Castiglione[3,4†], Elena Balestri[1*], Lucia Giorgetti[5], Stefania Bottega[3], Carlo Sorce[3,4], Carmelina Spanò[3,4§], Claudio Lardicci[2,4,6§]

[1]Department of Biology, University of Pisa, via Derna 1, 56126 Pisa, Italy

[2]Center for Instrument Sharing University of Pisa (CISUP), University of Pisa, via S. Maria 53, Pisa, Italy

[3]Department of Biology, University of Pisa, via L. Ghini 13, 56126 Pisa, Italy

[4]Center for Climate Change Impact, University of Pisa, Via Del Borghetto 80, Pisa, Italy

[5]Institute of Agricultural Biology and Biotechnology, (IBBA-CNR), Pisa, Italy

[6]Department of Earth Sciences, University of Pisa, via S. Maria 53, Pisa, Italy

**Corresponding author*

elena.balestri@unipi.it

† V. Menicagli and M. Ruffini Castiglione equally contributed

§ C. Spanò and C. Lardicci equally contributed

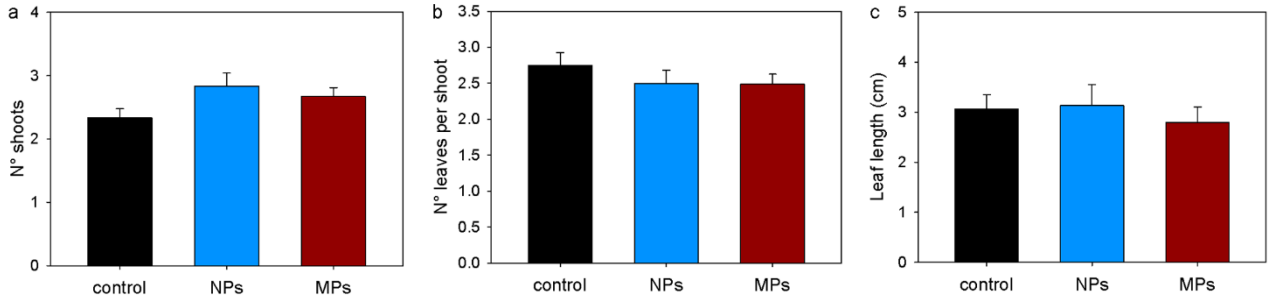

Fig. S1 Initial number of shoots (a), number of leaves per shoot (b), and leaf length (c) of *Cymodocea nodosa* plants grown in control condition (ctrl, without plastic) or treated by NPs or MPs. Values are means ± SE. n = 12.

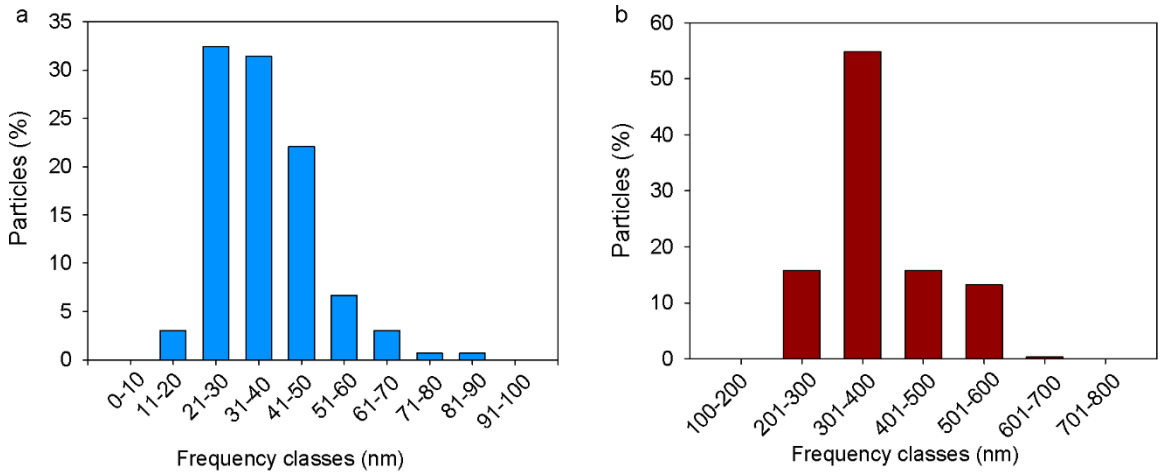

Fig. S2 Size distribution of polystyrene nanoparticles (a) and microparticles (b) grouped in frequency classes after an ImageJ program elaboration of SEM images.

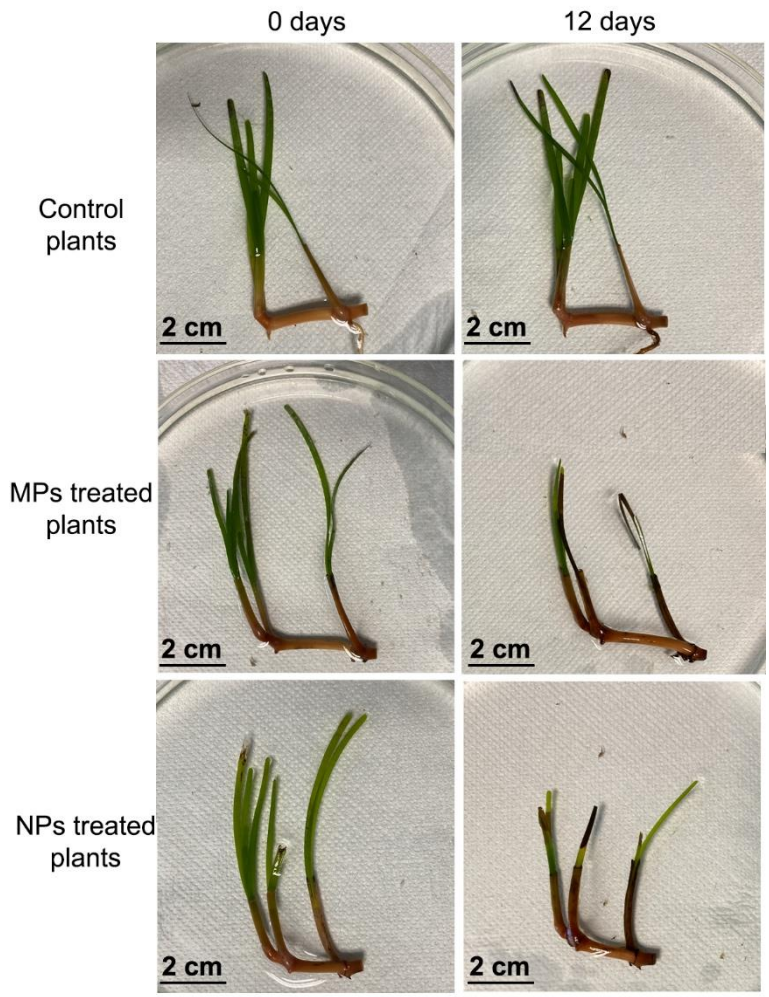

Fig. S3 Cuttings of *Cymodocea nodosa* at the beginning (0 days) and at the end (12 days) of the experiment exposed to different experimental conditions (i.e., plants grown in control or without plastic particles, plants grown with MPs, or plants grown with NPs).

Table S1 Results of ANOVA analysis on initial number of *Cymodocea nodosa* shoots, number of leaves per shoot and leaf length of plants grown without plastic or treated by NPs or MPs. A non-parametric Kruskal-Wallis test was performed on the number of shoots as data did not meet ANOVA assumptions.

N° shoots: Kruskal-Wallis Chi squared; χ^2: 4.05, df = 2, p = 0.131
N° leaves per shoot: $F_{2,33}$= 0.78 p = 0.463
Leaf length: $F_{2,33}$= 0.25 p = 0.773